Supporting information

Extended Charge-Accumulation in Ruthenium-4*H*-Imidazole based Black Absorbers - A Theoretical Design Concept

Stephan Kupfer[1,*]

[1]Institute of Physical Chemistry and Abbe Center of Photonics, Friedrich-Schiller-University Jena, Helmholtzweg 4, 07743 Jena, Germany

Corresponding author:
stephan.kupfer@uni-jena.de

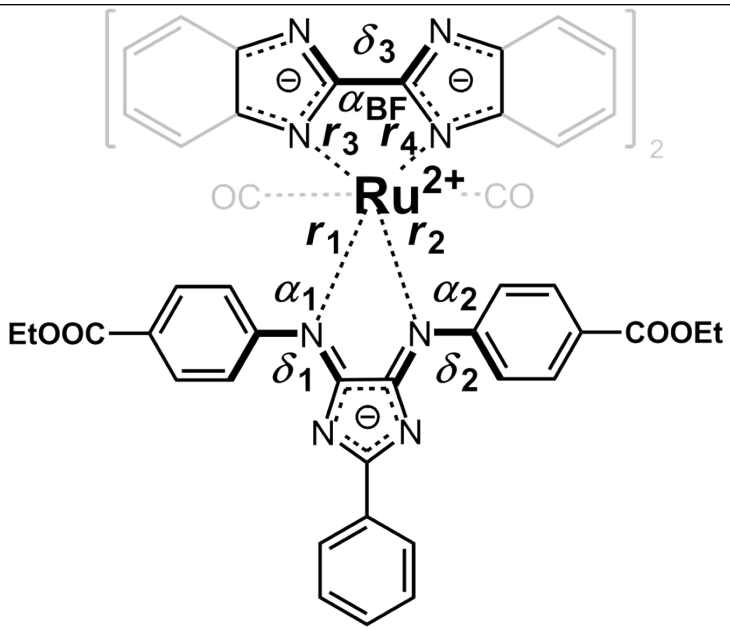

	4*H*-Imidazol						Bimidazole			
	r_1 / Å	r_2 / Å	α_1 / °	α_2 / °	δ_1 / °	δ_2 / °	r_3 / Å	r_4 / Å	α_{BF} / °	δ_3 / °
Ru 1	2.20	2.20	170.6	169.6	58	-52	2.15	2.14	25.7	1
Ru 2	2.19	2.19	178.7	178.3	69	-64	2.12	2.12	0.2	1
Ru 3	2.17	2.13	177.9	177.6	42	-45	2.13 2.12	2.12 2.14	0.6 0.8	1 1
Ru 4	2.10	2.16	174.9	174.2	44	-30	2.10 2.12	2.11 2.12	0.0 0.5	0 2

Table S1: Structural parameters of the 4*H*-imidazole (bond lengths: r_1 and r_2, pyramidalization: α_1 and α_2, torsion of the terminal phenyl moieties with respect to central 4*H*-imidazole plane: δ_1 and δ_2) and the bi(benz)imidazole ligand (bond lengths: r_3 and r_4, butterfly angle: α_{BF}, torsion of the two imidazole moieties: δ_3) in the fully optimized singlet ground state equilibrium structures of the complexes **Ru1**, **Ru2**, **Ru3** and **Ru4**.

Ru1					
State	Transition	Weight / %	E^e / eV	λ / nm	f
S_3	$\pi_{bim}+d_{xy}$ (203) → π^*_{im}(206)	99	2.22	557	0.063
S_4	$\pi_{im}+d_{xz}$(202) → π^*_{im}(206)	96	2.59	479	0.197
S_{13}	$\pi_{im}+d_{xy}$(199) → π^*_{im}(206)	85	3.26	380	0.506
S_{29}	π_{bim}(205) → π^*_{bim}(211)	79	3.83	324	0.606
Ru2					
State	Transition	Weight / %	E^e / eV	λ / nm	f
S_4	$d_{xz}+\pi_{im}$(178) → π^*_{im}(180)	98	2.50	495	0.109
S_8	$\pi_{bim}+d_{xy}$(177) → π^*_{im}(180)	98	2.87	431	0.253
S_9	π_{bim}(174) → π^*_{im}(180)	55	3.13	396	0.099
	π_{bim}(175) → π^*_{im}(180)	41			
S_{10}	π_{bim}(175) → π^*_{im}(180)	56	3.25	381	0.056
	π_{bim}(174) → π^*_{im}(180)	43			
S_{16}	π_{im}(172) → π^*_{im}(180)	66	3.56	348	0.233
	π_{bim}(179) → π^*_{im}(185)	14			
	π_{im}(168) → π^*_{im}(180)	10			
S_{17}	π_{bim}(179) → π^*_{im}(185)	46	3.56	348	0.052
	π_{im}(172) → π^*_{im}(180)	19			
	$d_{xz}+\pi_{im}$(178) → $\pi^*_{im}+\pi^*_{CO}$(181)	13			
	π_{bim}(179) → $d_{x^2-y^2}$(190)	11			
Ru3					
State	Transition	Weight / %	E^e / eV	λ / nm	f
S_3	d_{xy}(250) → π_{im}^*(253)	91	1.66	749	0.180
S_8	π_{bim}(247) → π_{im}^*(253)	76	2.45	505	0.050
	d_{yz}(251) → π_{im}^*(254)	21			
S_9	$\pi_{delocal}$(246) → π_{im}^*(253)	94	2.51	495	0.120
S_{10}	d_{xz}(252) → π_{im}^*(255)	90	2.54	489	0.043
S_{14}	d_{xy}(250) → π_{im}^*(255)	53	2.83	438	0.181
	d_{xz}(252) → π_{bim}^*(256)	29			
	$\pi_{delocal}$(244) → π_{im}^*(253)	10			
S_{16}	$\pi_{delocal}$(244) → π_{im}^*(253)	53	2.86	433	0.126
	d_{xz}(252) → π_{bim}^*(256)	20			
S_{18}	d_{yz}(251) → π_{bim}^*(256)	59	2.99	415	0.080
	$\pi_{delocal}$(243) → π_{im}^*(253)	17			
	d_{yz}(251) → π_{bim}^*(257)	17			
S_{37}	π_{im}(240) → π_{im}^*(253)	76	3.55	350	0.147
S_{48}	π_{bim}(249) → π_{bim}^*(256)	87	3.81	325	0.137
S_{51}	π_{bim}(249) → π_{bim}^*(257)	67	3.85	322	0.255
	π_{bim}(248) → π_{bim}^*(256)	17			
S_{52}	π_{bim}(248) → π_{bim}^*(256)	67	3.87	320	0.440
	π_{bim}(249) → π_{bim}^*(257)	15			
	π_{bim}(248) → π_{bim}^*(257)	10			
S_{55}	π_{bim}(248) → π_{bim}^*(257)	83	3.91	317	0.491
Ru4					
State	Transition	Weight / %	E^e / eV	λ / nm	f
S_3	$d_{xy}+\pi_{bim}$(199) → π^*_{im}(201)	77	1.32	938	0.049
	$d_{xy}+\pi_{bim}$(197) → π^*_{im}(201)	9			
	$d_{yz}+\pi_{bim}$(200) → π^*_{im}(201)	9			
S_5	$d_{xy}+\pi_{bim}$(197) → π^*_{im}(201)	87	1.81	684	0.168
S_{10}	π_{im}(195) → π^*_{im}(201)	71	2.63	472	0.278
	$d_{xy}+\pi_{bim}$(199) → π^*_{im}(203)	23			
S_{12}	$d_{xy}+\pi_{bim}$(199) → π^*_{im}(203)	64	2.70	459	0.233
	π_{im}(195) → π^*_{im}(201)	24			
S_{15}	$d_{xy}+\pi_{bim}$(197) → π^*_{im}(203)	90	3.05	406	0.101
S_{22}	$\pi_{delocal}$(191) → π^*_{im}(201)	89	3.33	372	0.149

Table S2: Calculated vertical excitation energies (E^e), wavelengths (λ) oscillator strengths (f), and singly-excited configurations of the main excited states in the visible range upon primary (singlet) photoexcitation within the respective optimized equilibrium geometry of **Ru1**, **Ru2**, **Ru3** and **Ru4**. The principal orbitals are depicted on Table S3.

Ru1

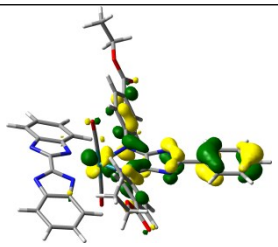

$\pi_{im}+d_{xv}(199)$

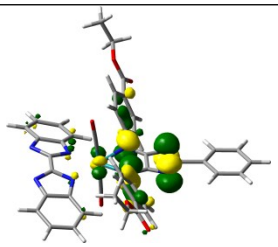

$\pi_{im}+d_{xz}(202)$

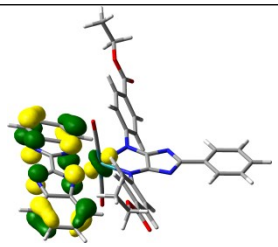

$\pi_{bim}+d_{xy}$ (203)

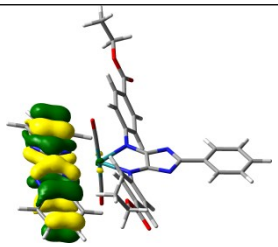

$\pi_{bim}(205)$

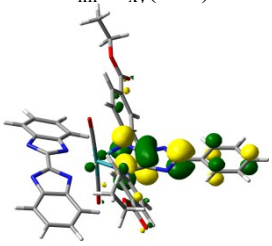

$\pi^*_{im}(206)$

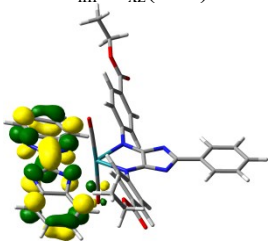

$\pi^*_{bim}(211)$

Ru2

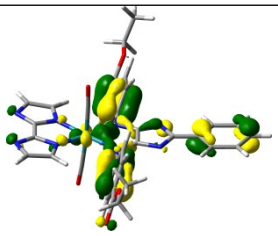

$\pi_{im}(168)$

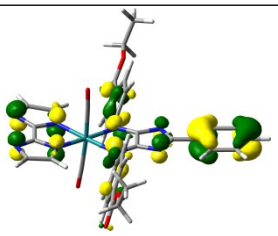

$\pi_{im}(172)$

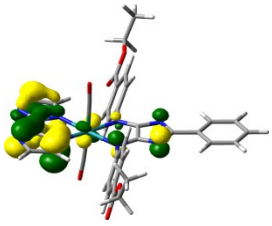

$\pi_{bim}(174)$

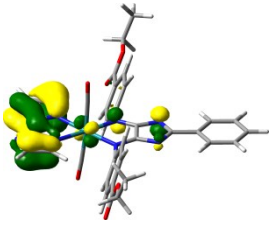

$\pi_{bim}(175)$

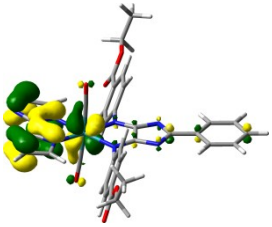

$\pi_{bim}+d_{xv}(177)$

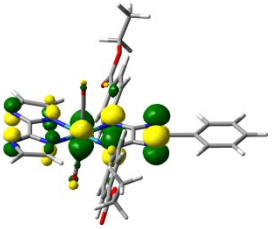

$d_{xz}+\pi_{im}(178)$

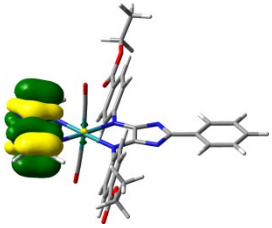

$\pi_{bim}(179)$

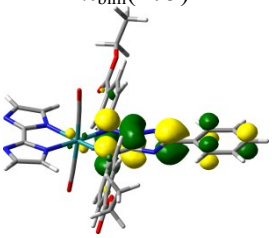

$\pi^*_{im}(180)$

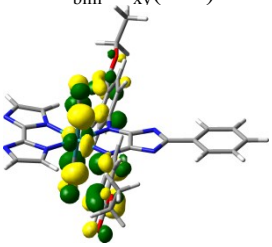

$\pi^*_{im}+\pi^*_{CO}(181)$

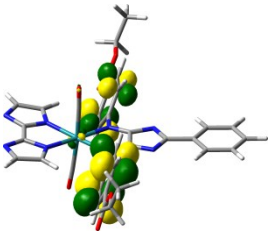

$\pi^*_{im}(185)$

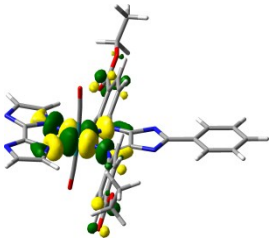

$d_{x^2-y^2}(190)$

Ru3

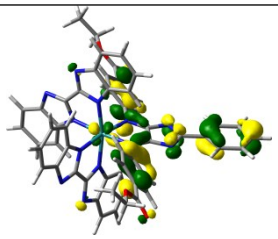

$\pi_{im}(240)$

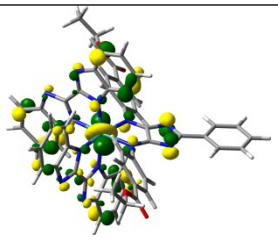

$\pi_{delocal}(243)$

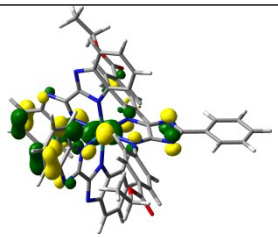

$\pi_{delocal}(244)$

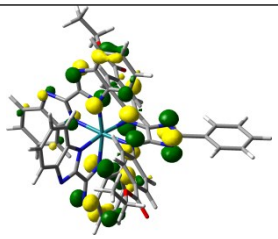

$\pi_{delocal}(246)$

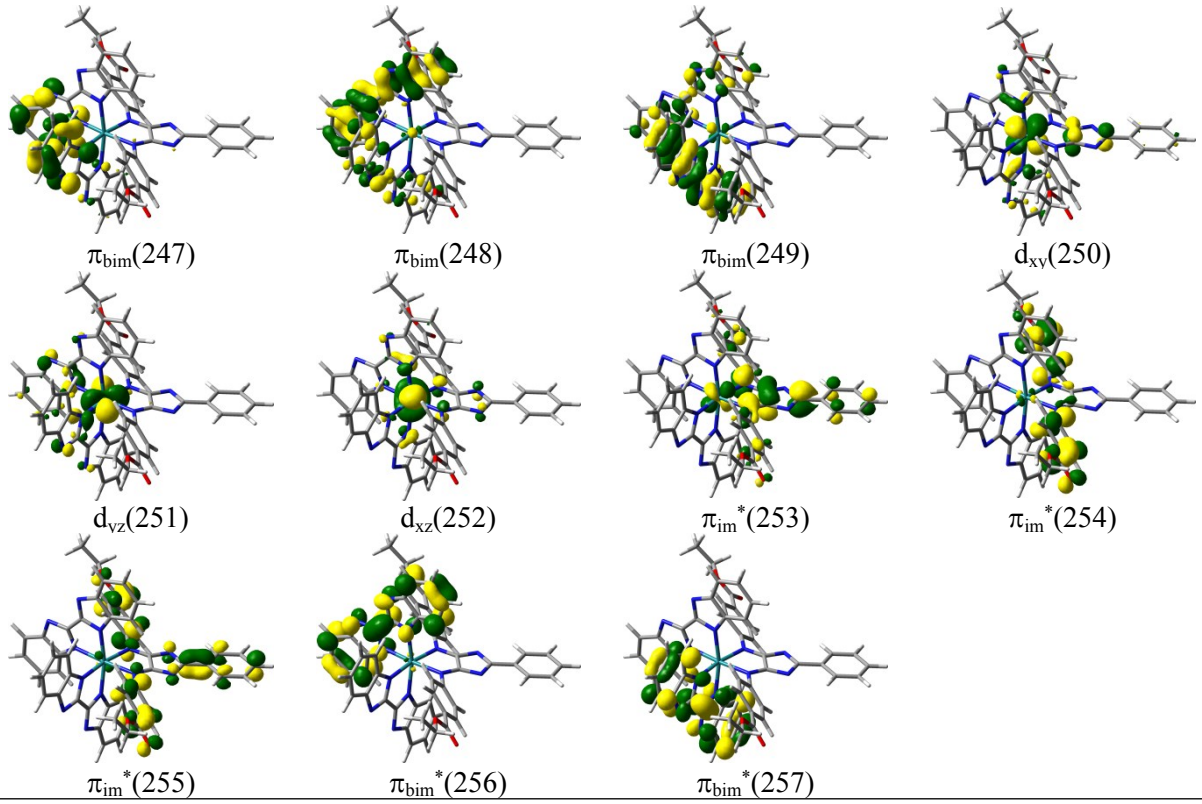

Ru4

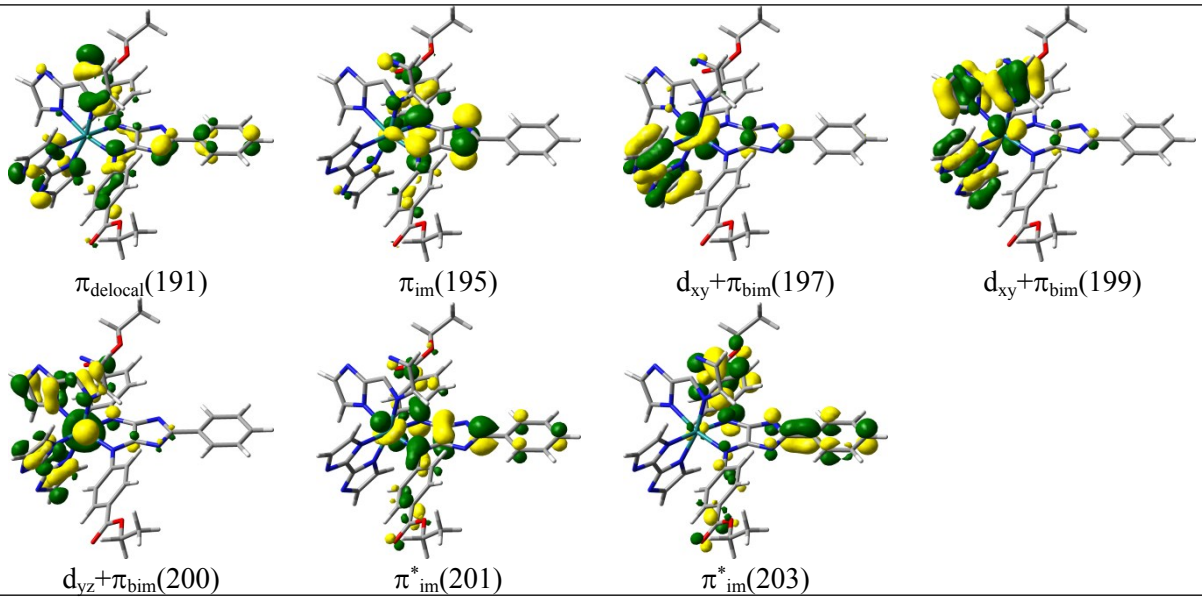

Table S3: MOs involved in the bright singlet excited states (Table S2) of **Ru1**, **Ru2**, **Ru3** and **Ru4** upon primary photoactivation.

Ru1 (singlet, S_0 geometry)

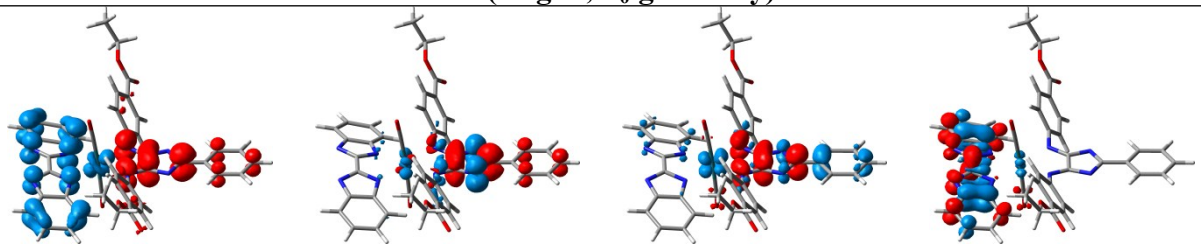

S_3 S_4 S_{13} S_{29}

Ru2 (singlet, S_0 geometry)

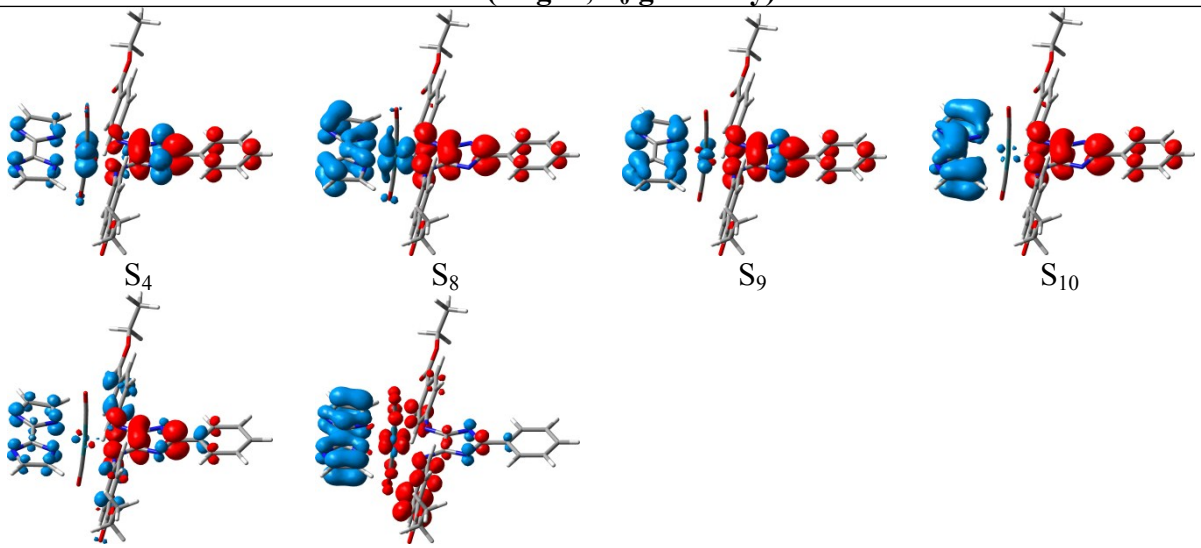

S_4 S_8 S_9 S_{10}

S_{16} S_{17}

Ru3 (singlet, S_0 geometry)

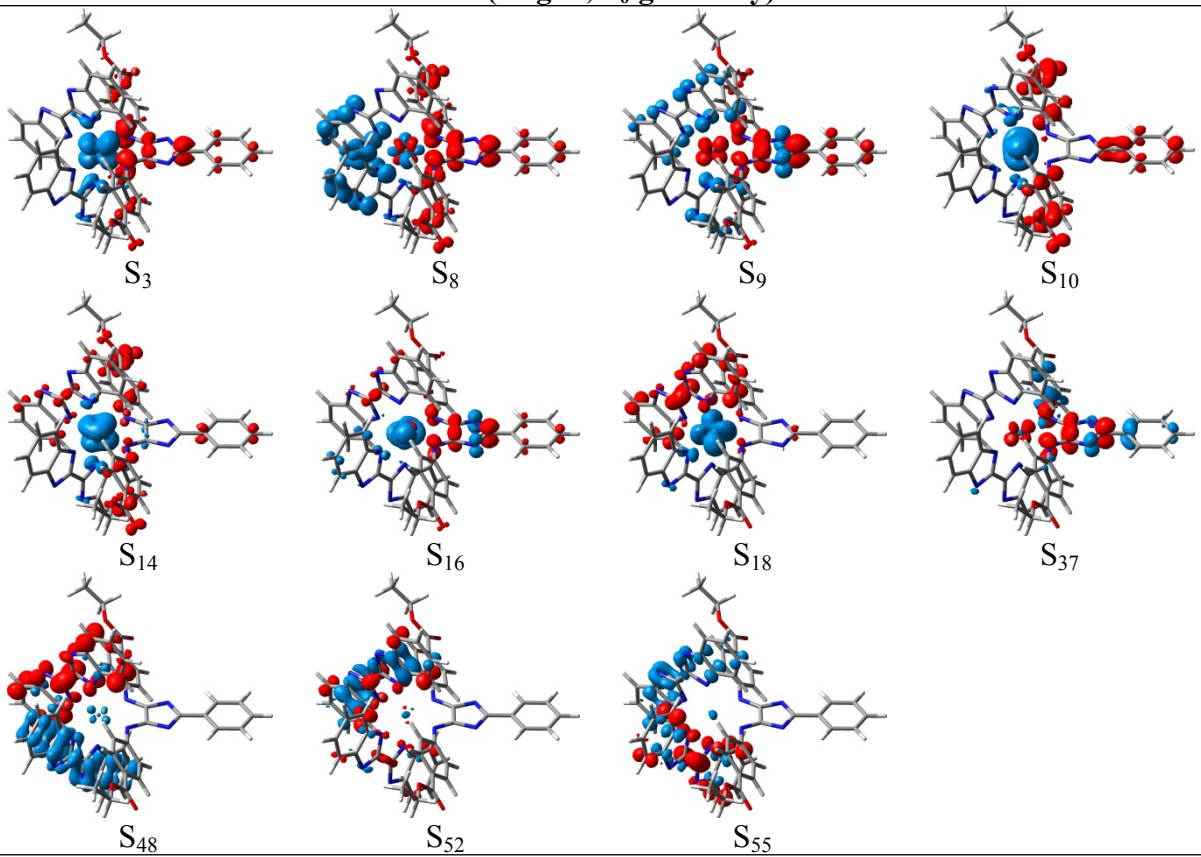

S_3 S_8 S_9 S_{10}

S_{14} S_{16} S_{18} S_{37}

S_{48} S_{52} S_{55}

Ru4 (singlet, S_0 geometry)			
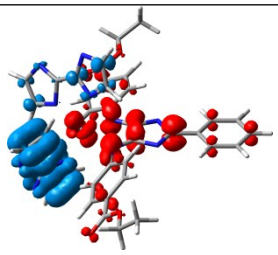 S_3	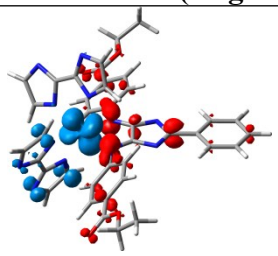 S_5	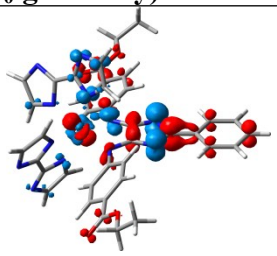 S_{10}	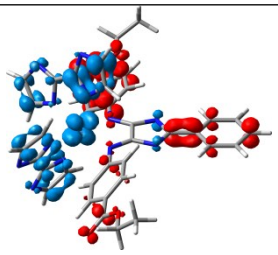 S_{12}
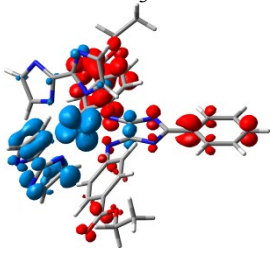 S_{15}	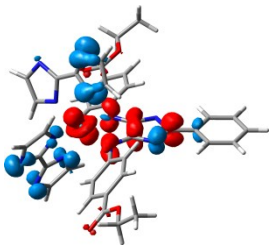 S_{22}		
Ru4 (triplet, T_1 geometry)			
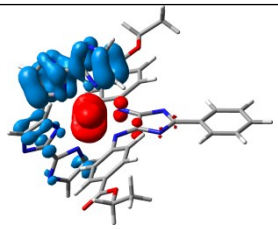 T_3	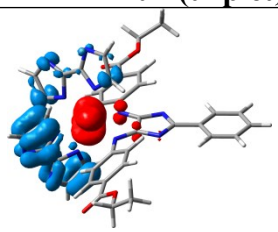 T_4	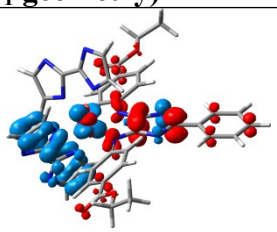 T_6	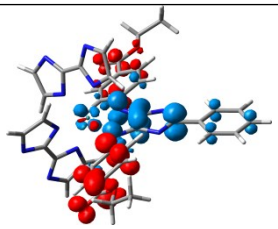 T_8
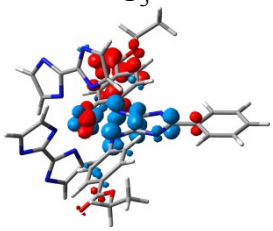 T_9	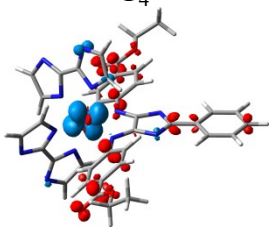 T_{11}	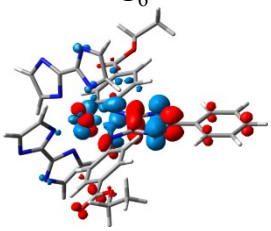 T_{12}	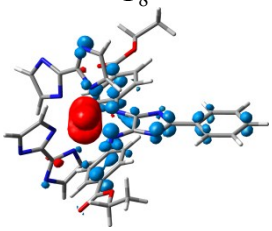 T_{14}

Table S4: CDDs for bright singlet excitations contributing to the UV-vis absorption spectrum of **Ru1**, **Ru2**, **Ru3** and **Ru4** as well as bright singlet excitations or **Ru4** within the respective optimized equilibrium structure. CT takes place from blue to red.

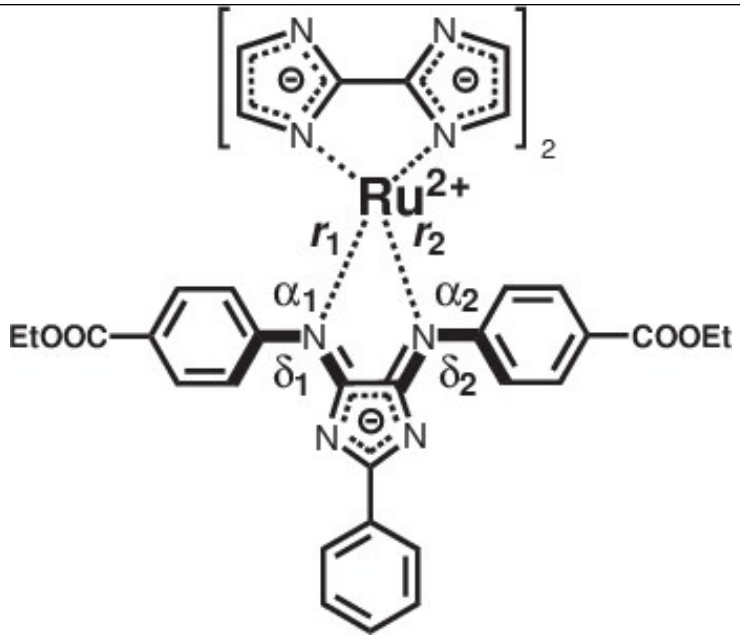

	E / eV	r_1 / Å	r_2 / Å	α_1 / °	α_2 / °	δ_1 / °	δ_2 / °
Single ox. doublet	3.15	2.16	2.15	178.4	177.3	49.1	-43.5
Non-red. singlet	0.00	2.10	2.16	174.9	174.2	43.5	-30.0
Non-red. triplet	0.23	2.15	2.16	177.9	175.6	31.2	-24.1
Single red. doublet	-2.42	2.18	2.15	160.8	167.2	0.5	18.2
Double red. singlet	-4.32	2.21	2.25	159.0	161.1	-1.6	-1.0
Double red. triplet	-3.26	2.24	2.07	166.9	173.6	-2.1	66.2

Table S5: Electronic ground state energies (*E*) and structural parameters (bond lengths: r_1 and r_2, pyramidalization: α_1 and α_2, torsion of the terminal phenyl moieties with respect to central 4*H*-imidazole plane: δ_1 and δ_2) for the non-reduced (singlet and triplet), the singly reduced (doublet) and doubly reduced species (singlet and triplet) of **Ru4**.

secondary photoexcitation (triplet, T_1 geometry)

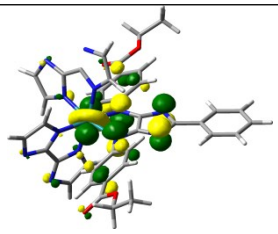
$d_{xz}(198\alpha)$

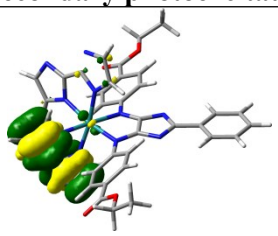
$\pi_{bim}(199\alpha)$

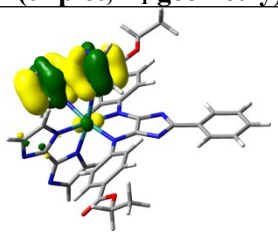
$\pi_{bim}(200\alpha)$

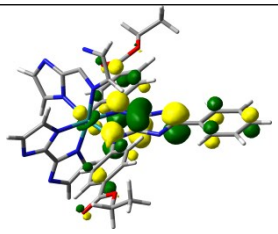
$\pi^*_{im}(201\alpha)$

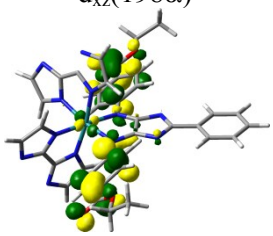
$\pi^*_{im}(202\alpha)$

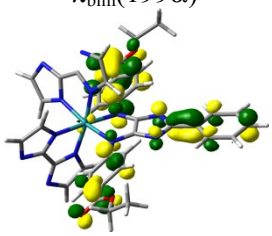
$\pi^*_{im}(203\alpha)$

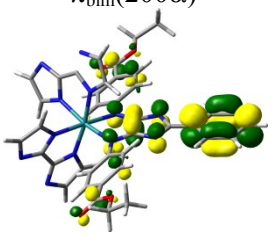
$\pi^*_{im}(204\alpha)$

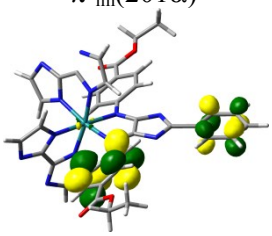
$\pi^*_{im}(205\alpha)$

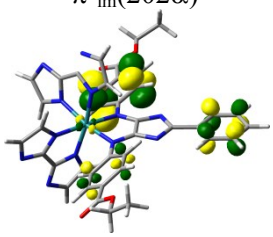
$\pi^*_{im}(207\alpha)$

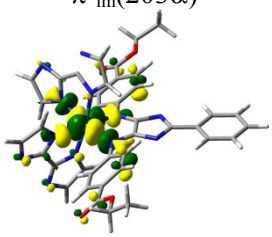
$d_{x^2y^2}(209\alpha)$

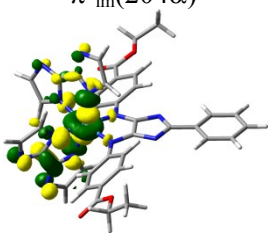
$d_{z^2}(210\alpha)$

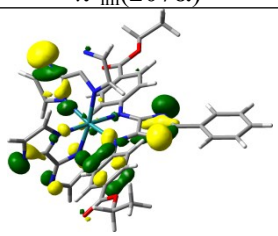
n(189β)

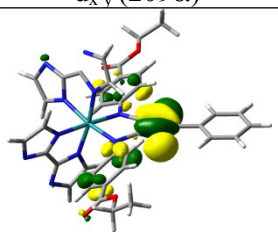
n(190β)

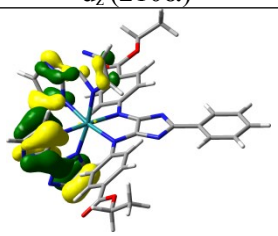
$\pi_{bim}(191\beta)$

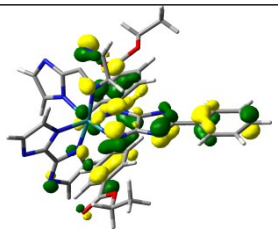
$\pi_{im}(194\beta)$

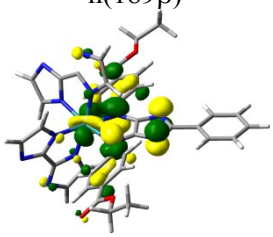
$\pi_{im}(195\beta)$

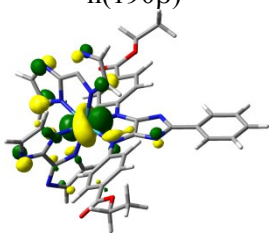
$d_{yz}(196\beta)$

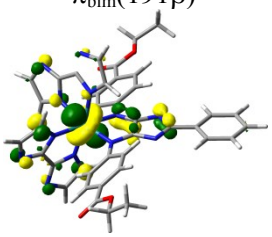
$d_{xy}(197\beta)$

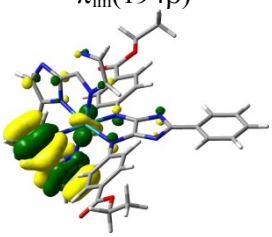
$\pi_{bim}(198\beta)$

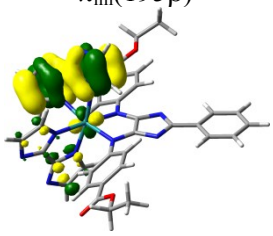
$\pi_{bim}(199\beta)$

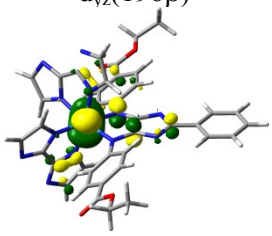
$d_{xz}(200\beta)$

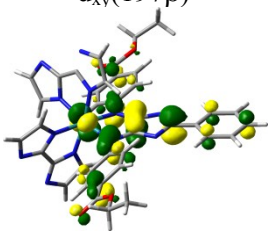
$\pi^*_{im}(201\beta)$

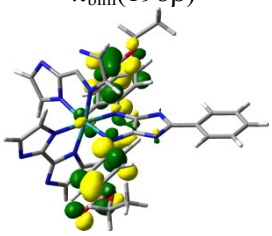
$\pi^*_{im}(202\beta)$

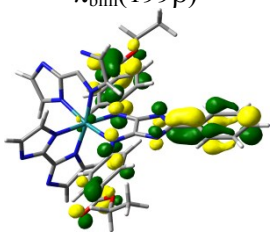
$\pi^*_{im}(203\beta)$

Table S6: MOs involved in the bright triplet excited states (Table 1) of **Ru4** upon secondary photoexcitation.

Singly oxidized (doublet)

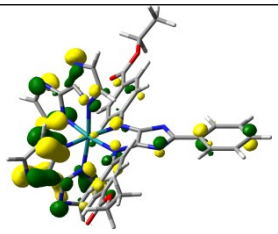
$\pi_{bim}(191\alpha)$

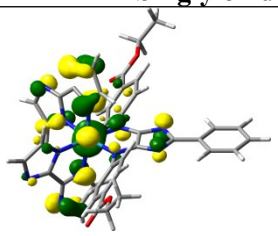
$\pi_{bim}+d_{xz}(195\alpha)$

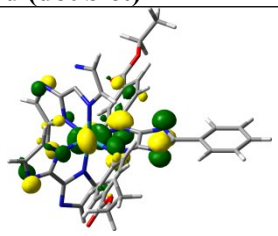
$d_{yz}+\pi_{im}(196\alpha)$

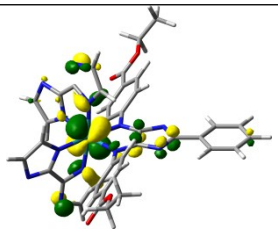
$d_{xy}(197\alpha)$

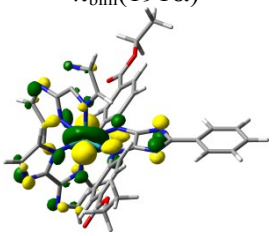
$d_{xz}+\pi_{bim}(198\alpha)$

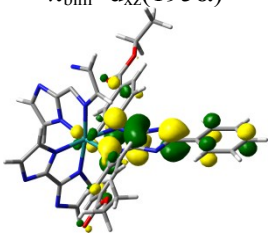
$\pi^*_{im}(201\alpha)$

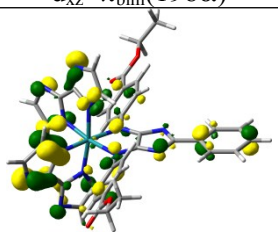
$\pi_{bim}(191\beta)$

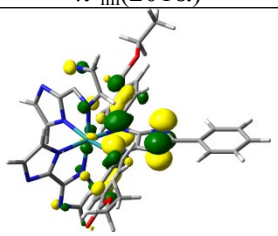
$\pi_{im}(195\beta)$

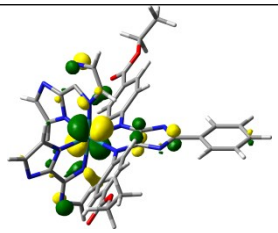
$d_{xy}(196\beta)$

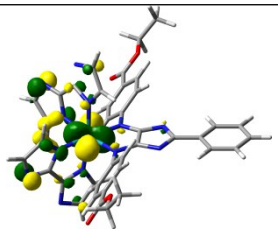
$d_{yz}(197\beta)$

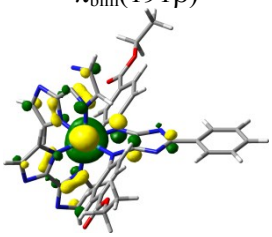
$d_{xz}(200\beta)$

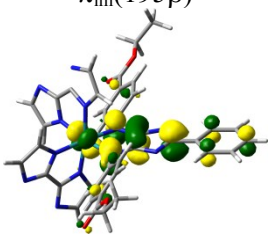
$\pi^*_{im}(201\beta)$

Singly reduced (doublet)

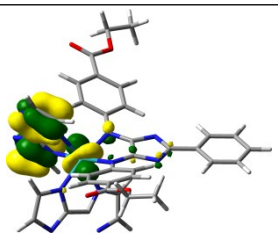
$\pi_{bim}(198\alpha)$

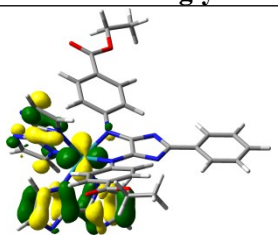
$d_{yz}+\pi_{bim}(199\alpha)$

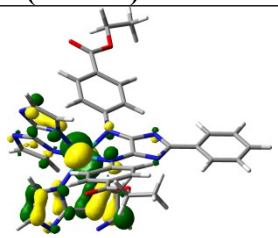
$d_{xz}+\pi_{bim}(200\alpha)$

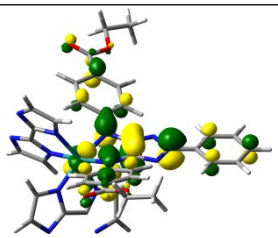
$\pi^*_{im}(201\alpha)$

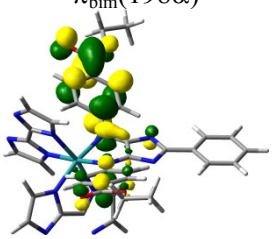
$\pi^*_{im}(202\alpha)$

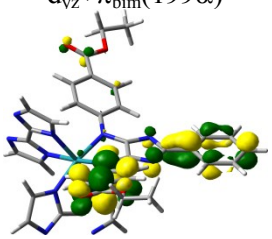
$\pi^*_{im}(203\alpha)$

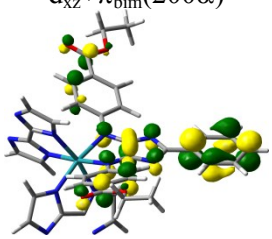
$\pi^*_{im}(204\alpha)$

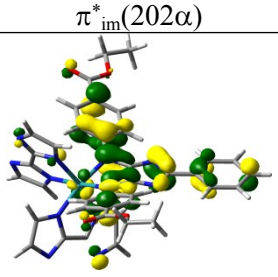

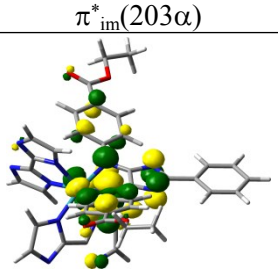

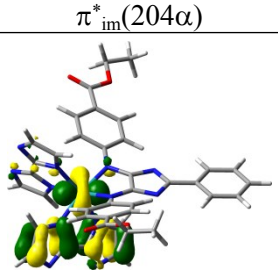

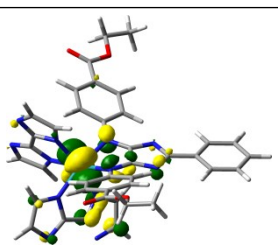

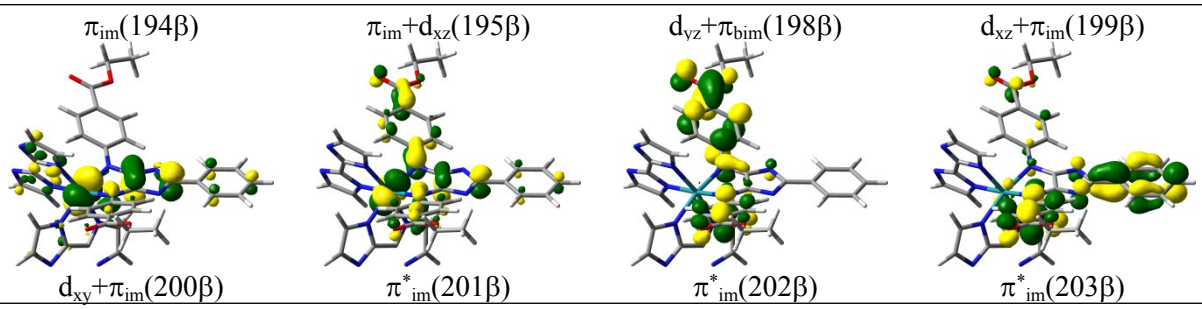

Doubly reduced (singlet)

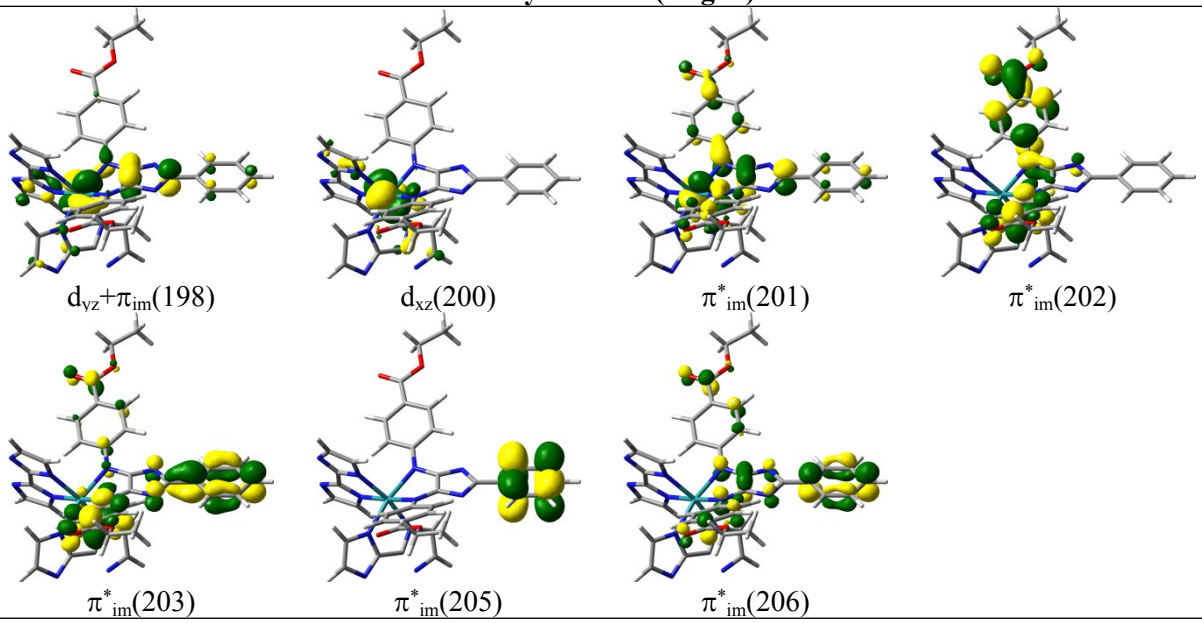

Doubly reduced (triplet)

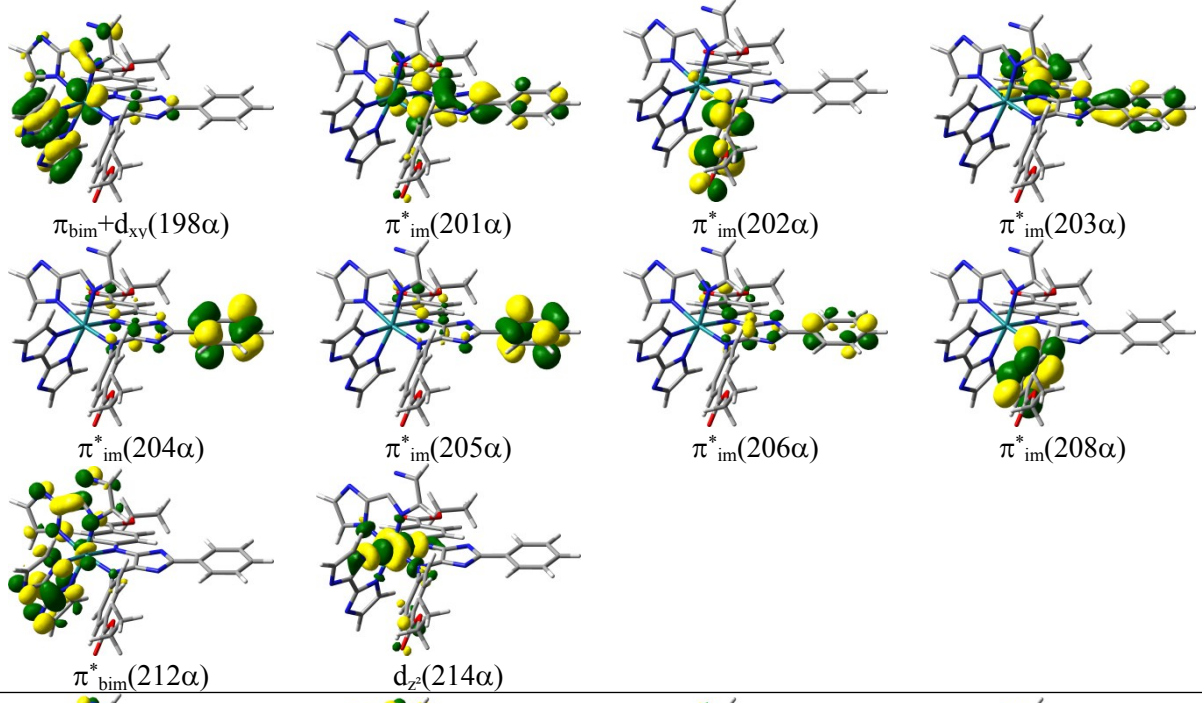

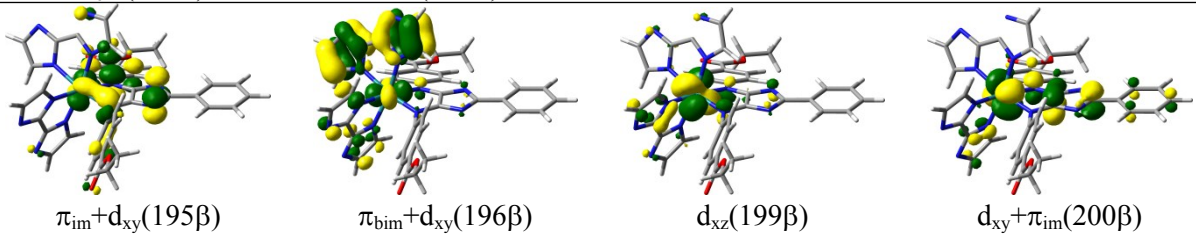

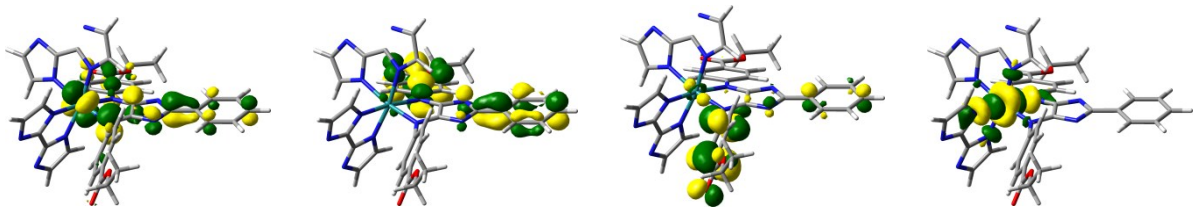

$d_{xy}+\pi^*_{im}(201\beta)$ $\pi^*_{im}(202\beta)$ $\pi^*_{im}(203\beta)$ $d_{z^2}(214\beta)$

Table S7: MOs involved in the bright excited states (Table S7) of **Ru4** in its singly oxidized (doublet), the singly reduced (doublet) and the doubly reduced (singlet and triplet) forms.

Singly oxidized (doublet)						
State	Transition	Weight / %	E^e / eV	λ / nm	f	$\langle S^2 \rangle$
D_{11}	$d_{xz}+\pi_{bim}(198\alpha) \rightarrow \pi^*_{im}(201\alpha)$	39	1.78	698	0.015	1.34
	$d_{yz}(197\beta) \rightarrow \pi^*_{im}(201\beta)$	33				
	$\pi_{im}(195\beta) \rightarrow \pi^*_{im}(201\beta)$	9				
	$d_{yz}+\pi_{im}(196\alpha) \rightarrow \pi^*_{im}(201\alpha)$	7				
D_{13}	$\pi_{im}(195\beta) \rightarrow d_{xz}(200\beta)$	40	2.19	565	0.032	0.92
	$d_{xy}(197\alpha) \rightarrow \pi^*_{im}(201\alpha)$	32				
	$\pi_{im}(195\beta) \rightarrow \pi^*_{im}(201\beta)$	8				
	$d_{xy}(196\beta) \rightarrow \pi^*_{im}(201\beta)$	8				
	$d_{yz}+\pi_{im}(196\alpha) \rightarrow \pi^*_{im}(201\alpha)$	8				
D_{14}	$\pi_{im}(195\beta) \rightarrow d_{xz}(200\beta)$	41	2.35	527	0.163	0.84
	$d_{xy}(197\alpha) \rightarrow \pi^*_{im}(201\alpha)$	34				
D_{15}	$\pi_{im}(195\beta) \rightarrow \pi^*_{im}(201\beta)$	48	2.51	494	0.160	1.24
	$d_{yz}+\pi_{im}(196\alpha) \rightarrow \pi^*_{im}(201\alpha)$	37				
	$\pi_{bim}+d_{xz}(195\alpha) \rightarrow \pi^*_{im}(201\alpha)$	10				
D_{46}	$\pi_{bim}(191\beta) \rightarrow \pi^*_{im}(201\beta)$	42	3.35	370	0.196	0.81
	$\pi_{bim}(191\alpha) \rightarrow \pi^*_{im}(201\alpha)$	40				
Singly reduced (doublet)						
State	Transition	Weight / %	E^e / eV	λ / nm	f	$\langle S^2 \rangle$
D_6	$\pi^*_{im}(201\alpha) \rightarrow \pi^*_{im}(202\alpha)$	78	1.77	701	0.177	1.13
D_7	$\pi^*_{im}(201\alpha) \rightarrow \pi^*_{im}(203\alpha)$	77	1.85	671	0.052	1.40
	$d_{xy}+\pi_{im}(200\beta) \rightarrow \pi^*_{im}(203\beta)$	12				
D_8	$\pi_{im}+d_{xz}(195\beta) \rightarrow \pi^*_{im}(201\beta)$	75	2.13	582	0.213	1.02
	$d_{xy}+\pi_{im}(200\beta) \rightarrow \pi^*_{im}(202\beta)$	17				
D_9	$d_{xy}+\pi_{im}(200\beta) \rightarrow \pi^*_{im}(202\beta)$	69	2.26	548	0.302	1.57
	$\pi_{im}+d_{xz}(195\beta) \rightarrow \pi^*_{im}(201\beta)$	10				
D_{10}	$d_{xy}+\pi_{im}(200\beta) \rightarrow \pi^*_{im}(203\beta)$	53	2.40	516	0.198	1.65
	$\pi^*_{im}(201\alpha) \rightarrow \pi^*_{im}(204\alpha)$	9				
	$\pi^*_{im}(201\alpha) \rightarrow \pi^*_{im}(203\alpha)$	9				
D_{11}	$d_{xz}+\pi_{im}(199\beta) \rightarrow \pi^*_{im}(202\beta)$	24	2.46	505	0.133	2.06
	$d_{xz}+\pi_{bim}(200\alpha) \rightarrow \pi^*_{im}(202\alpha)$	21				
	$d_{xy}+\pi_{im}(200\beta) \rightarrow \pi^*_{im}(203\beta)$	20				
D_{18}	$d_{yz}+\pi_{bim}(199\alpha) \rightarrow \pi^*_{im}(202\alpha)$	37	2.76	449	0.088	0.86
	$d_{yz}+\pi_{bim}(198\beta) \rightarrow \pi^*_{im}(202\beta)$	31				
	$d_{xz}+\pi_{im}(199\beta) \rightarrow \pi^*_{im}(203\beta)$	12				
	$d_{xz}+\pi_{bim}(200\alpha) \rightarrow \pi^*_{im}(203\alpha)$	10				
D_{26}	$\pi_{im}(194\beta) \rightarrow \pi^*_{im}(201\beta)$	73	2.93	424	0.120	1.01
	$\pi_{bim}(198\alpha) \rightarrow \pi^*_{im}(202\alpha)$	10				
Doubly reduced (singlet)						
State	Transition	Weight / %	E^e / eV	λ / nm	f	$\langle S^2 \rangle$
S_1	$\pi^*_{im}(201) \rightarrow \pi^*_{im}(202)$	46	2.00	621	0.392	-
	$\pi^*_{im}(201) \rightarrow \pi^*_{im}(203)$	41				
S_2	$\pi^*_{im}(201) \rightarrow \pi^*_{im}(202)$	47	2.03	612	0.345	-
	$\pi^*_{im}(201) \rightarrow \pi^*_{im}(203)$	47				
S_4	$d_{xz}(200 \rightarrow \pi^*_{im}(203)$	75	2.31	537	0.219	-
	$d_{xz}(200) \rightarrow \pi^*_{im}(202)$	8				
S_9	$d_{yz}+\pi_{im}(198) \rightarrow \pi^*_{im}(202)$	70	2.56	485	0.306	-
	$\pi^*_{im}(201) \rightarrow \pi^*_{im}(205)$	20				
S_{10}	$d_{yz}+\pi_{im}(198) \rightarrow \pi^*_{im}(203)$	84	2.67	464	0.283	-
S_{11}	$\pi^*_{im}(201) \rightarrow \pi^*_{im}(206)$	64	2.73	454	0.191	-
Doubly reduced (triplet)						
State	Transition	Weight / %	E^e / eV	λ / nm	f	$\langle S^2 \rangle$
T_6	$\pi^*_{im}(201\alpha) \rightarrow \pi^*_{im}(203\alpha)$	81	1.55	802	0.114	2.61
	$d_{xy}+\pi_{im}(200\beta) \rightarrow (202\beta)$	13				
T_7	$\pi^*_{im}(202\alpha) \rightarrow \pi^*_{im}(204\alpha)$	47	1.61	768	0.042	2.04
	$\pi^*_{im}(202\alpha) \rightarrow \pi^*_{im}(205\alpha)$	24				
	$\pi^*_{im}(202\alpha) \rightarrow \pi^*_{im}(208\alpha)$	18				
T_9	$\pi^*_{im}(202\alpha) \rightarrow \pi^*_{im}(206\alpha)$	84	1.68	737	0.024	2.03
	$\pi^*_{im}(202\alpha) \rightarrow \pi^*_{im}(208\alpha)$	9				
T_{14}	$d_{xy}+\pi_{im}(200\beta) \rightarrow (202\beta)$	35	2.23	556	0.267	2.75
	$\pi_{bim}+d_{xy}(196\beta) \rightarrow (201\beta)$	21				
	$\pi^*_{im}(201\alpha) \rightarrow \pi^*_{im}(203\alpha)$	10				

T_{21}	$\pi_{im}+d_{xy}(195\beta) \rightarrow (201\beta)$ $\pi^*_{im}(201\alpha) \rightarrow \pi^*_{im}(206\alpha)$ $\pi^*_{im}(200\alpha) \rightarrow \pi^*_{im}(203\alpha)$	29 20 14	2.52	492	0.120	2.34
T_{23}	$\pi^*_{im}(202\alpha) \rightarrow \pi^*_{bim}(212\alpha)$ $d_{xy}+\pi_{im}(200\beta) \rightarrow (203\beta)$	44 22	2.58	481	0.092	2.21
T_{25}	$d_{xz}(199\beta) \rightarrow (202\beta)$ $\pi^*_{im}(202\alpha) \rightarrow d_{z^2}(214\alpha)$ $d_{xz}(199\beta) \rightarrow d_{z^2}(214\beta)$	27 10 9	2.65	468	0.081	2.85
T_{33}	$\pi_{bim}+d_{xy}(198\alpha) \rightarrow \pi^*_{im}(203\alpha)$	56	2.86	434	0.098	2.63

Table S8: Calculated vertical excitation energies (E^e), wavelengths (λ) oscillator strengths (f), eigen values of $\langle s^2 \rangle$ and singly-excited configurations of the main excited states in the visible range for the singly oxidized (doublet), the singly reduced (doublet) and the doubly reduced (singlet and triplet) of **Ru4** within the respective optimized equilibrium geometry. Involved MOs are depicted on Table S7.

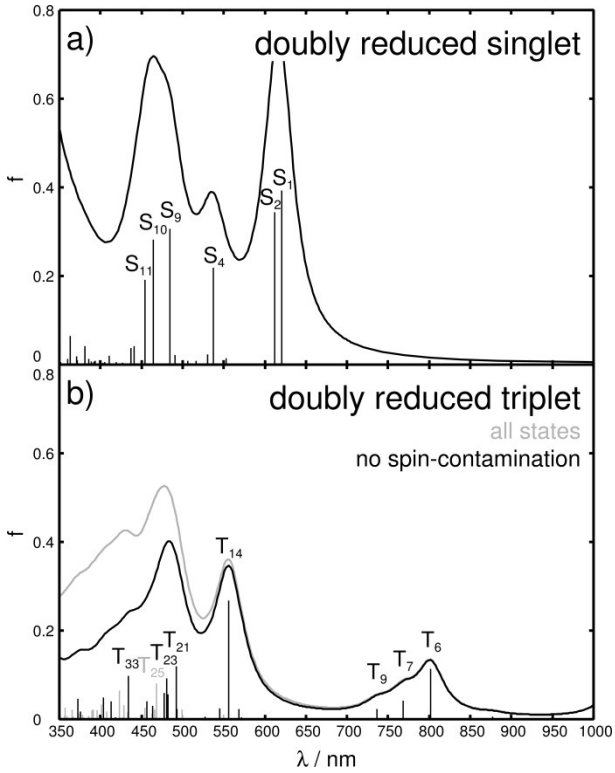

Figure S1: Calculated absorption spectra of the doubly reduced singlet (a) and triplet (b) species of **Ru4**. Spin-contaminated states of the doubly reduced triplet species, b), with $\langle s^2 \rangle \leq s(s+1) + 0.75$ are given in grey.

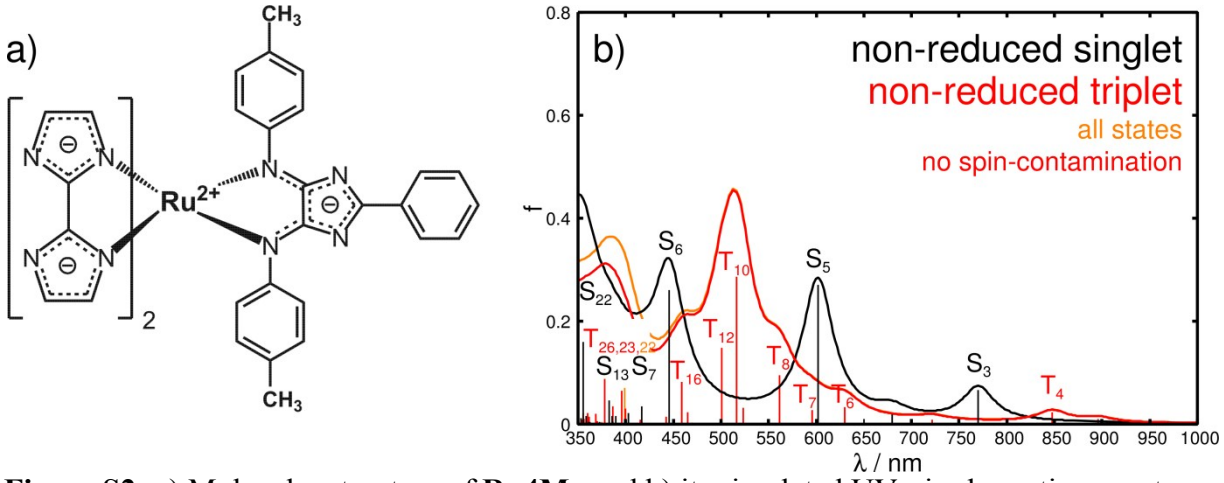

Figure S2: a) Molecular structure of **Ru4Me** and b) its simulated UV-vis absorption spectrum upon primary (singlet) and secondary photoexcitation (triplet-to-triplet). Spin-contaminated states of the non- reduced triplet species, b), with $\langle s^2 \rangle \leq s(s+1) + 0.75$ are given in orange.

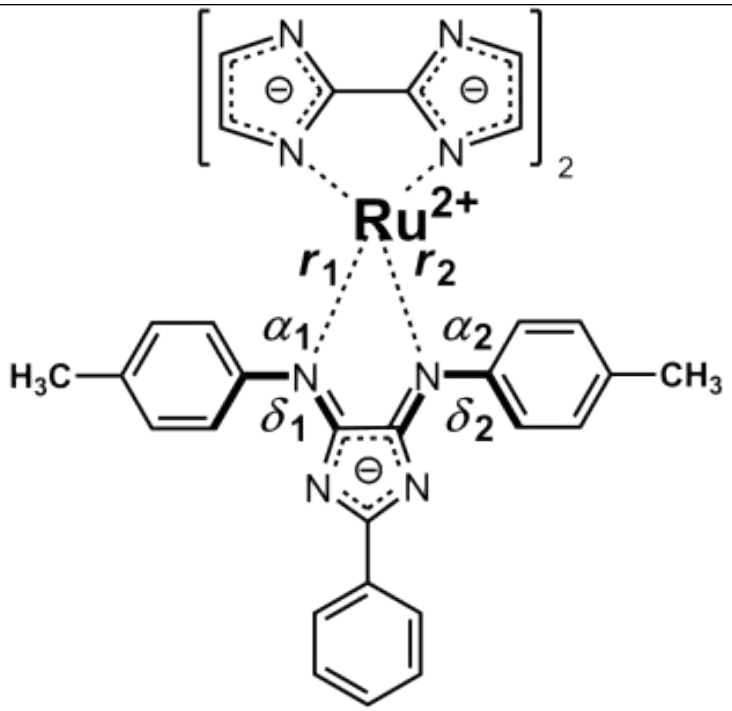

	E / eV	r_1 / Å	r_2 / Å	α_1 / °	α_2 / °	δ_1 / °	δ_2 / °
Non-red. singlet	0.00	2.11	2.15	175.4	175.3	48.1	-36.2
Non-red. triplet	0.39	2.13	2.14	178.7	177.1	38.7	-30.6
Double red. singlet	-3.31	2.26	2.26	162.0	171.1	7.9	9.1
Double red. triplet	-1.96	2.23	2.22	161.4	168.4	17.2	12.3.2

Table S9: Electronic ground state energies (*E*) and structural parameters (bond lengths: r_1 and r_2, pyramidalization: α_1 and α_2, torsion of the terminal phenyl moieties with respect to central 4*H*-imidazole plane: δ_1 and δ_2) for the non-reduced (singlet and triplet), the singly reduced (doublet) and doubly reduced species (singlet and triplet) of **Ru4Me**.

primary photoexcitation (singlet, S_0 geometry)

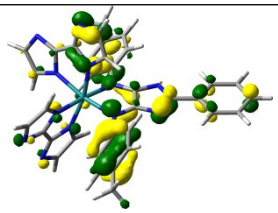
$\pi_{delocal}(162)$

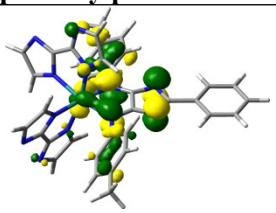
$\pi_{im}(165)$

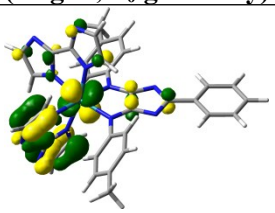
$d_{xv}+\pi_{bim}(167)$

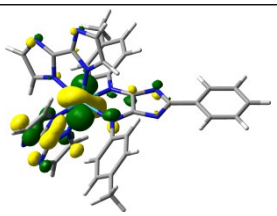
$d_{yz}(168)$

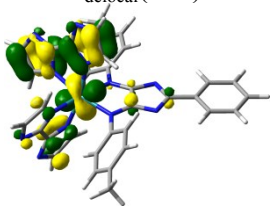
$d_{xy}+\pi_{bim}(169)$

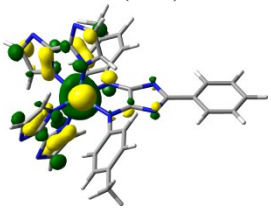
$d_{xz}(170)$

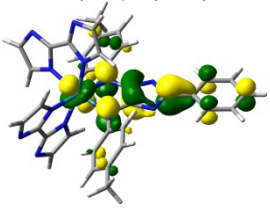
$\pi^*_{im}(171)$

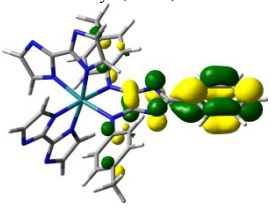
$\pi^*_{im}(172)$

secondary photoexcitation (triplet, T_1 geometry)

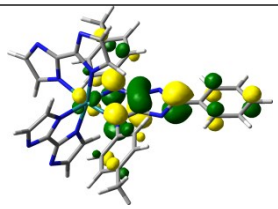
$\pi^*_{im}(171\alpha)$

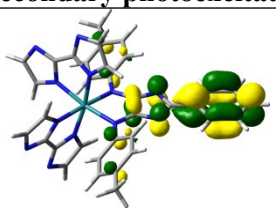
$\pi^*_{im}(172\alpha)$

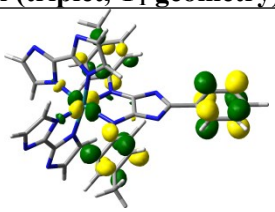
$\pi^*_{im}+d_{x^2-y^2}(173\alpha)$

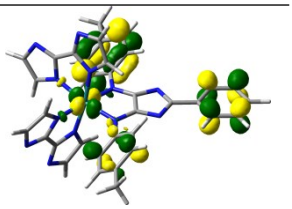
$\pi^*_{im}+d_{x^2-y^2}(175\alpha)$

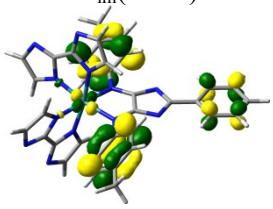
$\pi^*_{im}(176\alpha)$

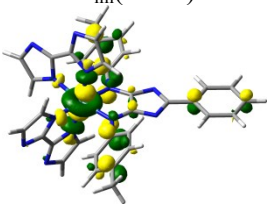
$d_{z^2}+\pi^*_{bim}(178\alpha)$

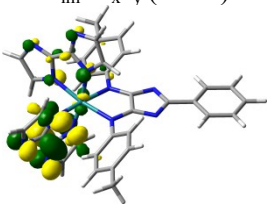
$\pi^*_{bim}(179\alpha)$

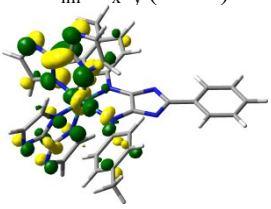
$\pi^*_{bim}(180\alpha)$

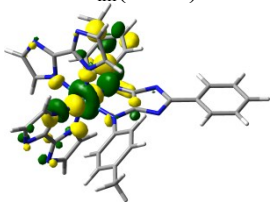
$d_{z^2}+\pi^*_{bim}(183\alpha)$

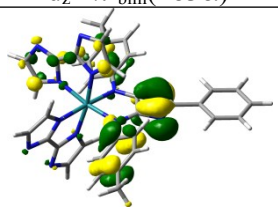
$n(161\beta)$

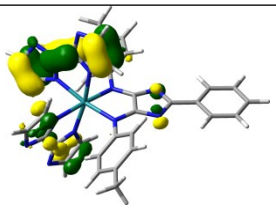
$\pi_{bim}(163\beta)$

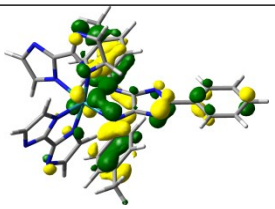
$\pi_{im}(164\beta)$

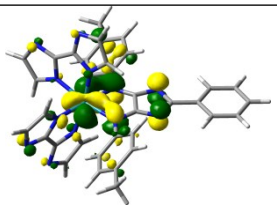
$d_{yz}+\pi_{im}(165\beta)$

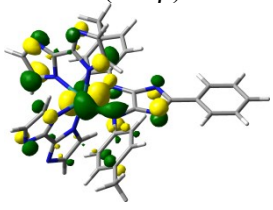
$d_{yz}+\pi_{im}(166\beta)$

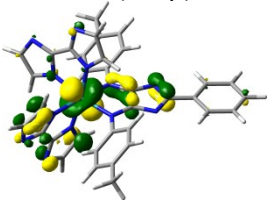
$d_{xy}(167\beta)$

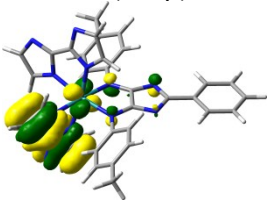
$\pi_{bim}(168\beta)$

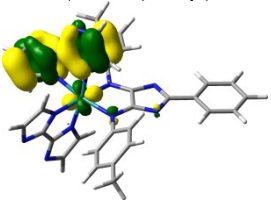
$\pi_{bim}(169\beta)$

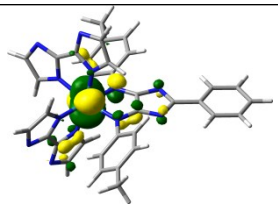
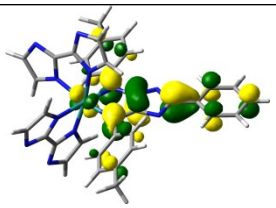

$d_{xz}(170\beta)$ $\pi^*_{im}(171\beta)$

Table S10: MOs involved in the bright singlet and triplet excited states (Table S11) of the methyl-substituted (4*H*-imidazole) **Ru4Me** upon primary and secondary photoexcitation.

primary photoexcitation (singlet, S_0 geometry)						
State	Transition	Weight / %	E^e / eV	λ / nm	f	$\langle S^2 \rangle$
S_3	$d_{xy}+\pi_{bim}(169) \rightarrow \pi^*_{im}(171)$ (MLCT)	60	1.61	770	0.066	0.00
	$d_{yz}(168) \rightarrow \pi^*_{im}(171)$ (MLCT)	22				
	$d_{xy}+\pi_{bim}(167) \rightarrow \pi^*_{im}(171)$ (MLCT)	14				
S_5	$d_{xy}+\pi_{bim}(167) \rightarrow \pi^*_{im}(171)$ (MLCT)	84	2.06	602	0.270	0.00
S_6	$\pi_{im}(165) \rightarrow \pi^*_{im}(171)$ (ILCT)	94	2.78	446	0.261	0.00
S_7	$d_{xz}(170) \rightarrow \pi^*_{im}(172)$ (MLCT)	91	2.97	417	0.034	0.00
S_{13}	$d_{xy}+\pi_{bim}(169) \rightarrow \pi^*_{im}(172)$ (MLCT)	69	3.24	383	0.046	0.00
S_{22}	$\pi_{delocal}(162) \rightarrow \pi^*_{im}(171)$ (LLCT/ILCT)	80	3.49	356	0.160	0.00
secondary photoexcitation (triplet, T_1 geometry)						
State	Transition	Weight / %	E^e / eV	λ / nm	f	$\langle S^2 \rangle$
T_4	$\pi_{bim}(168\beta) \rightarrow d_{xz}(170\beta)$ (LMCT)	52	1.46	848	0.023	2.04
	$d_{yz}+\pi_{im}(166\beta) \rightarrow d_{xz}(170\beta)$ (MC/LMCT)	14				
	$d_{yz}+\pi_{im}(165\beta) \rightarrow d_{xz}(170\beta)$ (MC/LMCT)	12				
	$d_{xy}(167\beta) \rightarrow d_{xz}(170\beta)$ (MC)	10				
	$\pi_{bim}(169\beta) \rightarrow d_{xz}(170\beta)$ (LMCT)	10				
T_6	$\pi_{bim}(169\beta) \rightarrow \pi^*_{im}(171\beta)$ (LLCT)	67	1.97	630	0.033	2.03
	$\pi_{bim}(168\beta) \rightarrow \pi^*_{im}(171\beta)$ (LLCT)	21				
	$d_{yz}+\pi_{im}(166\beta) \rightarrow \pi^*_{im}(171\beta)$ (MLCT)	9				
T_7	$\pi_{bim}(168\beta) \rightarrow \pi^*_{im}(171\beta)$ (LLCT)	54	2.08	596	0.027	2.03
	$\pi_{bim}(169\beta) \rightarrow \pi^*_{im}(171\beta)$ (LLCT)	17				
T_8	$\pi^*_{im}(171\alpha) \rightarrow \pi^*_{im}(172\alpha)$ (ILCT)	64	2.21	561	0.094	2.06
	$d_{xy}(167\beta) \rightarrow \pi^*_{im}(171\beta)$ (MLCT)	10				
	$\pi_{bim}(168\beta) \rightarrow \pi^*_{im}(171\beta)$ (LLCT)	9				
	$\pi_{bim}(169\beta) \rightarrow \pi^*_{im}(171\beta)$ (LLCT)	8				
T_{10}	$d_{xy}(167\beta) \rightarrow \pi^*_{im}(171\beta)$ (MLCT)	60	2.40	517	0.286	2.03
	$\pi^*_{im}(171\alpha) \rightarrow \pi^*_{im}(172\alpha)$ (IL)	18				
T_{12}	$\pi^*_{im}(171\alpha) \rightarrow \pi^*_{im}+d_{x^2-y^2}(173\alpha)$ (ILCT)	29	2.47	501	0.148	2.16
	$\pi^*_{im}(171\alpha) \rightarrow \pi^*_{im}+d_{x^2-y^2}(175\alpha)$ (ILCT)	25				
	$d_{yz}+\pi_{im}(165\beta) \rightarrow \pi^*_{im}(171\beta)$ (MLCT)	15				
	$d_{yz}+\pi_{im}(166\beta) \rightarrow \pi^*_{im}(171\beta)$ (MLCT)	9				
T_{16}	$\pi^*_{im}(171\alpha) \rightarrow \pi^*_{im}(176\alpha)$ (ILCT)	52	2.70	459	0.081	2.07
	$\pi_{im}(164\beta) \rightarrow d_{xz}(170\beta)$ (LMCT)	31				
	$\pi^*_{im}(171\alpha) \rightarrow \pi^*_{im}+d_{x^2-y^2}(175\alpha)$ (ILCT)	10				
T_{22}	$\pi_{bim}(163\beta) \rightarrow d_{xz}(170\beta)$ (LMCT)	27	3.11	399	0.071	2.80
	$\pi^*_{im}(171\alpha) \rightarrow d_{z^2}+\pi^*_{bim}(183\alpha)$ (LMCT)	12				
	$\pi^*_{im}(171\alpha) \rightarrow \pi^*_{bim}(180\alpha)$ (LLCT)	8				
T_{23}	$n(161\beta) \rightarrow d_{xz}(170\beta)$ (LMCT)	45	3.13	396	0.064	2.37
	$\pi_{im}(164\beta) \rightarrow \pi^*_{im}(171\beta)$ (ILCT)	10				
T_{26}	$\pi_{im}(164\beta) \rightarrow \pi^*_{im}(171\beta)$ (ILCT)	31	3.28	378	0.087	2.41
	$\pi^*_{im}(171\alpha) \rightarrow \pi^*_{bim}(179\alpha)$ (LLCT)	10				
	$\pi^*_{im}(171\alpha) \rightarrow d_{z^2}+\pi^*_{bim}(178\alpha)$ (LMCT)	9				

Table S11: Calculated vertical excitation energies (E^e), wavelengths (λ) oscillator strengths (f), eigen values of $\langle s^2 \rangle$ and singly-excited configurations of the main excited states in the visible range upon primary (singlet) and secondary photoexcitation within the respective optimized equilibrium geometry of **Ru4Me**. The principal orbitals are depicted on Table S10.

Doubly reduced singlet	Doubly reduced triplet	
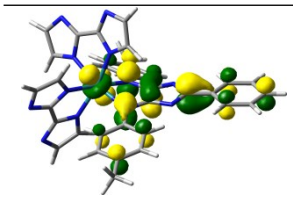	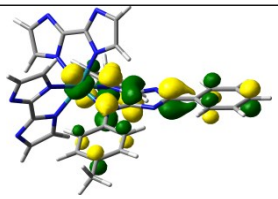	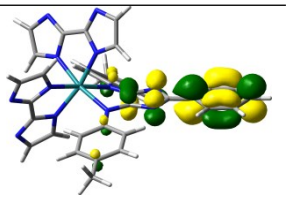
$\pi^*_{im}(171)$	$\pi^*_{im}(171\alpha)$	$\pi^*_{im}(172\alpha)$

Table S12: Frontier orbitals of the doubly reduced singlet and triplet forms of **Ru4Me** collecting two electrochemical introduced excess.

Character	non-reduced triplet			singly oxidized			singly reduced		
	State	E^e / eV	f	State	E^e / eV	f	State	E^e / eV	f
ILCT ($\pi_{im} \rightarrow \pi^*_{im}$)	T_{12}	2.27	0.340	D_{15}	2.51	0.161	D_8	2.13	0.213
ILCT ($\pi^*_{im} \rightarrow \pi^*_{im}$)	T_8	1.90	0.243		-		D_6	1.77	0.177
	T_9	1.99	0.039		-		D_7	1.85	0.052
	T_{11}	2.13	0.191		-		D_8	2.13	0.213
LMCT (charge-recombination)	T_6	1.68	0.017	D_{11}	1.78	0.015		-	
	T_9	1.99	0.039	D_{13}	2.19	0.032		-	
	T_{14}	2.75	0.132	D_{14}	2.35	0.163		-	

Table S13: Comparison of electronic excitations (excitation energy E^e and oscillator strength f) of corresponding character between the non-reduced triplet (secondary photoexcitation) and the singly oxidized/reduced species of **Ru4**. ILCT states of $\pi^*_{im} \rightarrow \pi^*_{im}$ nature are not present in the singly oxidized species (no excess charge on 4*H*-imidazole), while LMCT charge-recombination states are not present in the singly reduced Ruthenium(II) species.

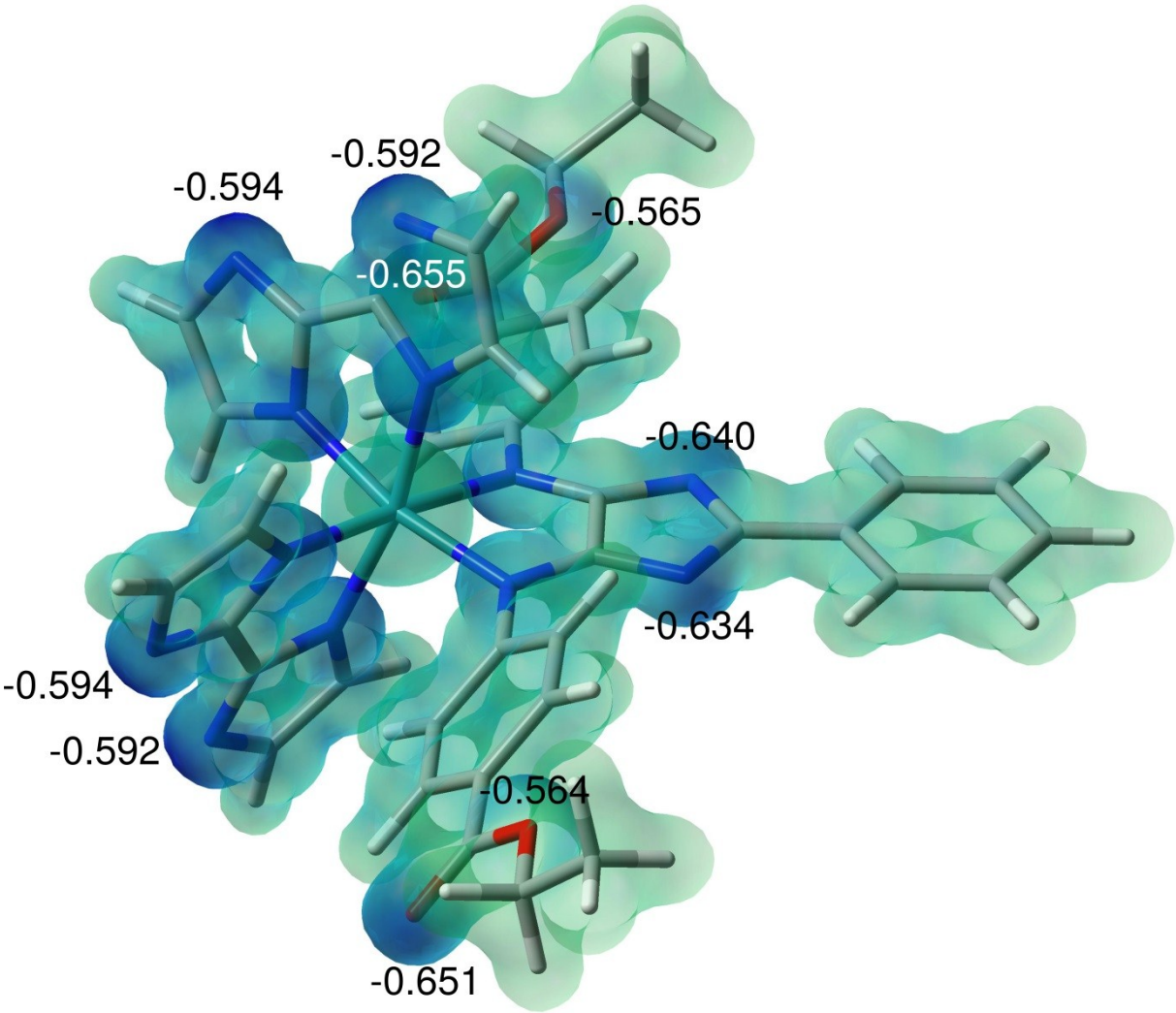

Figure S3: Electrostatic potential on top of total electron density and charge distribution based on NBO analysis for potential protonation sites.

		ΔE / eV	ΔG / eV	q_i	r_1 / Å	r_2 / Å	α_1 / °	α_2 / °	δ_1 / °	δ_2 / °
Bimidazole	Singlet	0.00	0.00	-0.594	2.11	2.15	177.0	176.6	47	-39
	Triplet	0.39	0.39		2.10	2.15	177.3	175.8	34	-25
4*H*-imidazole	Singlet	0.49	0.53	-0.640	2.07	2.15	176.3	178.0	50	-42
	Triplet	0.60	0.63		2.17	2.16	177.5	176.6	37	-38
Carbonyle	Singlet	2.01	2.01	-0.655	2.03	2.23	172.7	169.2	51	-5
	Triplet	2.06	2.00		2.14	2.19	178.1	174.7	38	-18

Table S14: Relative electronic ground state energies (ΔE) and relative free energy (ΔG) as well as structural parameters (bond lengths: r_1 and r_2, pyramidalization: α_1 and α_2, torsion of the terminal phenyl moieties with respect to central 4*H*-imidazole plane: δ_1 and δ_2) with respect to single protonation at the biimidazolate, the 4*H*-imidazole and the carbonyl group of **Ru4**. Partial charges of these three groups (q_i), obtained by means of NBO analysis, are given within the non-protonated equilibrium structure.

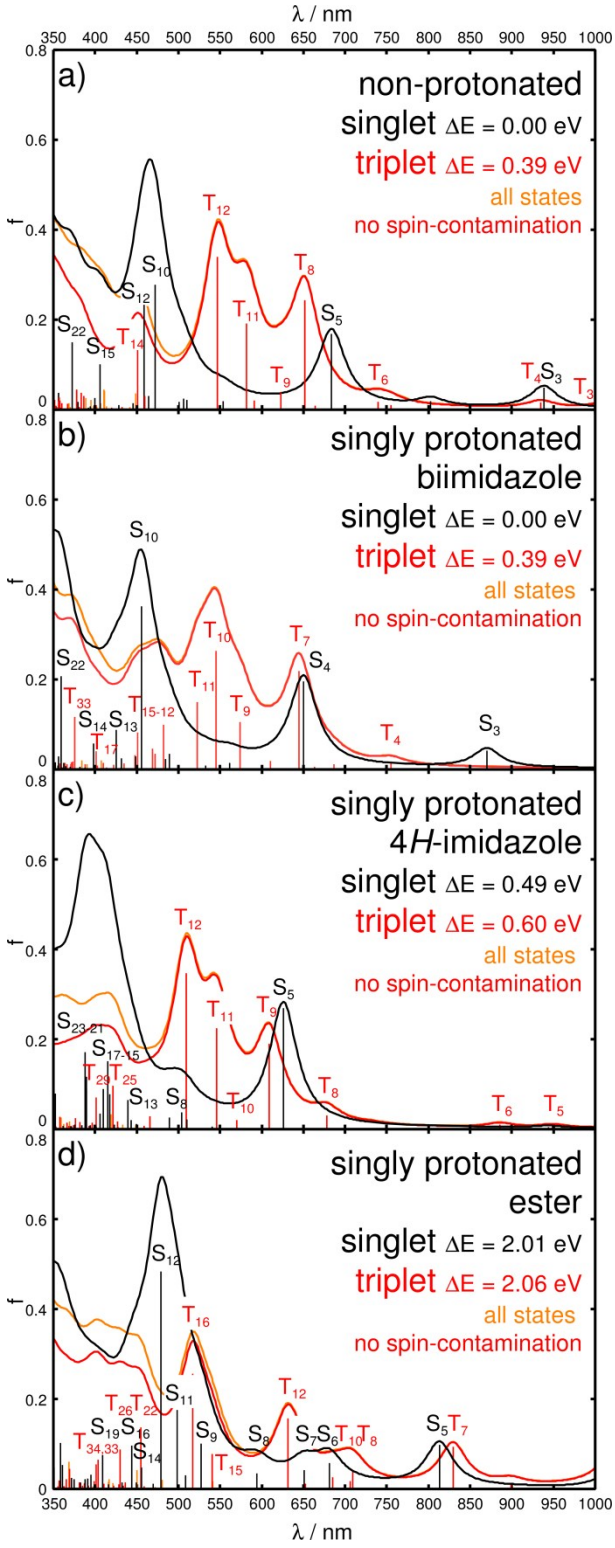

Figure S4: Simulated UV-vis absorption spectrum upon primary (singlet) and secondary photoexcitation (triplet-to-triplet) for, a), **Ru4** (non-protonated, recall Figure 3b) and respective singly protonated species, b), protonated at non-coordinating biimidazole nitrogen atoms, c), at 4*H*-imidazole and, d), at carbonyl group. For open-shell systems (triplet) all states as well as those states within a threshold for spin-contamination of $\langle s^2 \rangle \leq s(s+1) + 0.75$ are given, see respective color code.

Single protonation: Biimidazole primary photoexcitation (singlet, S_0 geometry)						
q_i		ΔE / eV			ΔG / eV	
-0.594		0.00			0.00	
State	Transition	Weight / %	E^e / eV	λ / nm	f	$\langle S^2 \rangle$
S_3	$d_{yz}+\pi_{bim}(198) \rightarrow \pi^*_{im}(201)$	31	1.42	870	0.042	-
	$d_{xz}(199) \rightarrow \pi^*_{im}(201)$	28				
	$\pi_{bim}(200) \rightarrow \pi^*_{im}(201)$	27				
	$d_{yz}+\pi_{bim}(197) \rightarrow \pi^*_{im}(201)$	14				
S_4	$d_{yz}+\pi_{bim}(197) \rightarrow \pi^*_{im}(201)$	79	1.91	650	0.195	-
	$d_{yz}+\pi_{bim}(198) \rightarrow \pi^*_{im}(201)$	16				
S_{10}	$\pi_{im}(195) \rightarrow \pi^*_{im}(201)$	80	2.72	456	0.363	-
	$d_{xz}(199) \rightarrow \pi^*_{im}(203)$	13				
S_{13}	$d_{yz}+\pi_{bim}(198) \rightarrow \pi^*_{im}(203)$	92	2.92	425	0.088	-
S_{14}	$d_{yz}+\pi_{bim}(197) \rightarrow \pi^*_{im}(203)$	87	3.11	398	0.057	-
S_{22}	$\pi_{delocal}(193) \rightarrow \pi^*_{im}(201)$	87	3.45	359	0.207	-
secondary photoexcitation (triplet, T_1 geometry)						
State	Transition	Weight / %	E^e / eV	λ / nm	f	$\langle S^2 \rangle$
T_3	$\pi_{bim}(199\beta) \rightarrow d_{xz}(200\beta)$	75	1.14	1088	0.021	2.04
	$d_{yz}+\pi_{im}(197\beta) \rightarrow d_{xz}(200\beta)$	16				
T_4	$\pi_{im}(196\beta) \rightarrow d_{xz}(200\beta)$	40	1.64	755	0.014	2.03
	$d_{yz}+\pi_{im}(197\beta) \rightarrow d_{xz}(200\beta)$	34				
	$\pi_{bim}(199\beta) \rightarrow \pi^*_{im}(201\beta)$	9				
T_5	$\pi_{bim}(199\beta) \rightarrow \pi_{im}{}^*(201\beta)$	41	1.80	687	0.012	2.04
	$\pi_{bim}+d_{yz}(195\beta) \rightarrow d_{xz}(200\beta)$	32				
	$d_{xy}+\pi_{bim}(198\beta) \rightarrow d_{xz}(200\beta)$	15				
T_7	$\pi^*_{im}(201\alpha) \rightarrow \pi^*_{im}(202\alpha)$	86	1.92	645	0.218	2.08
T_9	$d_{xy}+\pi_{bim}(198\beta) \rightarrow \pi^*_{im}(201\beta)$	64	2.16	574	0.105	2.04
	$\pi^*_{im}(201\alpha) \rightarrow \pi^*_{im}(203\alpha)$	11				
	$d_{yz}+\pi_{im}(197\beta) \rightarrow \pi^*_{im}(201\beta)$	11				
T_{10}	$d_{yz}+\pi_{im}(197\beta) \rightarrow \pi^*_{im}(201\beta)$	67	2.27	545	0.264	2.04
	$\pi^*_{im}(201\alpha) \rightarrow \pi^*_{im}(203\alpha)$	14				
T_{11}	$\pi_{im}(196\beta) \rightarrow \pi^*_{im}(201\beta)$	89	2.37	523	0.150	2.04
T_{12}	$\pi_{im}(194\beta) \rightarrow d_{xz}(200\beta)$	86	2.57	483	0.100	2.04
T_{13}	$\pi^*_{im}(201\alpha) \rightarrow \pi^*_{bim}(204\alpha)$	48	2.63	472	0.035	2.24
	$\pi_{bim}+d_{yz}(195\beta) \rightarrow \pi^*_{im}(201\beta)$	17				
	$\pi^*_{im}(201\alpha) \rightarrow d_{z^2}(209\alpha)$	14				
T_{14}	$\pi_{bim}+d_{yz}(195\beta) \rightarrow \pi^*_{im}(201\beta)$	72	2.64	469	0.045	2.10
	$\pi^*_{im}(201\alpha) \rightarrow \pi^*_{bim}(204\alpha)$	12				
T_{15}	$\pi^*_{im}(201\alpha) \rightarrow \pi^*_{im}(205\alpha)$	65	2.75	451	0.082	2.28
T_{17}	$\pi_{bim}(193\beta) \rightarrow d_{xz}(200\beta)$	91	2.85	434	0.013	2.11
T_{33}	$\pi_{im}(194\beta) \rightarrow \pi^*_{im}(201\beta)$	20	3.30	376	0.116	2.66
	$\pi_{bim}+\pi_{im}(198\alpha) \rightarrow \pi^*_{im}(202\alpha)$	13				
	$\pi_{bim}+\pi_{im}(199\alpha) \rightarrow \pi^*_{im}(202\alpha)$	12				
	$\pi_{bim}(199\beta) \rightarrow \pi^*_{im}(203\beta)$	9				

Table S15: Calculated vertical excitation energies (E^e), wavelengths (λ), oscillator strengths (f), eigen values of $\langle s^2 \rangle$ and singly-excited configurations of the main excited states in the visible range upon primary (singlet) and secondary photoexcitation (triplet) within the respective optimized equilibrium geometry of **Ru4** singly protonated at the bibenzimidazole. The MOs involved in the electronic transitions are depicted on Table S18.

Single protonation: 4*H*-imidazole primary photoexcitation (singlet, S_0 geometry)						
q_i		ΔE / eV			ΔG / eV	
-0.640		0.49			0.53	
State	Transition	Weight / %	E^e / eV	λ / nm	f	$\langle S^2 \rangle$
S_5	$d_{xy}(196) \rightarrow \pi^*_{im}(201)$	48	1.98	626	0.269	-
	$d_{yz}(197) \rightarrow \pi^*_{im}(201)$	46				
S_8	$\pi_{bim}(199) \rightarrow \pi^*_{im}(202)$	60	2.46	504	0.037	-
	$\pi_{bim}(200) \rightarrow \pi^*_{im}(203)$	32				
S_{13}	$\pi_{bim}(194) \rightarrow \pi^*_{im}(201)$	74	2.82	439	0.064	-
	$d_{xz}(198) \rightarrow \pi^*_{im}(203)$	12				
	$\pi_{bim}(195) \rightarrow \pi^*_{im}(201)$	9				
S_{15}	$\pi_{bim}(192) \rightarrow \pi^*_{im}(201)$	30	2.97	418	0.077	-
	$\pi_{delocal}(193) \rightarrow \pi^*_{im}(201)$	27				
	$\pi_{bim}(195) \rightarrow \pi^*_{im}(202)$	26				
S_{16}	$\pi_{bim}(192) \rightarrow \pi^*_{im}(201)$	61	2.98	416	0.150	-
	$\pi_{delocal}(193) \rightarrow \pi^*_{im}(201)$	22				
S_{17}	$d_{xy}(196) \rightarrow \pi^*_{im}(202)$	68	3.03	410	0.090	-
	$d_{yz}(197) \rightarrow \pi^*_{im}(202)$	8				
	$d_{xy}(196) \rightarrow \pi^*_{im}(203)$	8				
S_{21}	$d_{xy}(196) \rightarrow \pi^*_{im}(203)$	36	3.18	390	0.116	-
	$n_{bim}(191) \rightarrow \pi^*_{im}(201)$	33				
	$\pi_{bim}(200) \rightarrow \pi^*_{im}(205)$	17				
S_{22}	$\pi_{bim}(200) \rightarrow \pi^*_{im}(205)$	66	3.18	390	0.089	-
	$n_{bim}(191) \rightarrow \pi^*_{im}(201)$	12				
S_{23}	$n_{bim}(190) \rightarrow \pi^*_{im}(201)$	84	3.19	388	0.171	-
secondary photoexcitation (triplet, T_1 geometry)						
State	Transition	Weight / %	E^e / eV	λ / nm	f	$\langle S^2 \rangle$
T_3	$\pi_{bim}(199\beta) \rightarrow d_{xz}+\pi^*_{im}(200\beta)$	74	1.06	1172	0.016	2.03
	$d_{xy}(196\beta) \rightarrow d_{xz}+\pi^*_{im}(200\beta)$	13				
T_4	$\pi_{bim}(198\beta) \rightarrow d_{xz}+\pi^*_{im}(200\beta)$	68	1.14	1086	0.022	2.03
	$d_{yz}(197\beta) \rightarrow d_{xz}+\pi^*_{im}(200\beta)$	14				
	$\pi_{bim}(198\beta) \rightarrow \pi^*_{im}+d_{xz}\ (201\beta)$	9				
T_5	$\pi_{bim}(199\beta) \rightarrow \pi^*_{im}+d_{xz}(201\beta)$	84	1.31	949	0.008	2.04
	$\pi_{bim}(199\beta) \rightarrow d_{xz}+\pi^*_{im}(200\beta)$	9				
T_6	$\pi_{bim}(198\beta) \rightarrow \pi^*_{im}+d_{xz}(201\beta)$	73	1.40	886	0.010	2.03
	$\pi_{bim}(198\beta) \rightarrow d_{xz}+\pi^*_{im}(200\beta)$	15				
T_8	$d_{xy}(196\beta) \rightarrow \pi^*_{im}+d_{xz}(201\beta)$	61	1.83	678	0.030	2.03
	$d_{xy}(196\beta) \rightarrow d_{xz}+\pi^*_{im}(200\beta)$	26				
T_9	$\pi^*_{im}(201\alpha) \rightarrow \pi^*_{im}(202\alpha)$	89	2.04	609	0.190	2.08
T_{10}	$\pi^*_{im}(201\alpha) \rightarrow \pi^*_{im}(203\alpha)$	59	2.17	570	0.020	2.10
	$\pi_{im}(195\beta) \rightarrow d_{xz}+\pi^*_{im}(200\beta)$	32				
T_{11}	$\pi_{im}(195\beta) \rightarrow d_{xz}+\pi^*_{im}(200\beta)$	61	2.27	546	0.225	2.04
	$\pi^*_{im}(201\alpha) \rightarrow \pi^*_{im}(203\alpha)$	25				
T_{12}	$\pi_{im}(195\beta) \rightarrow \pi^*_{im}+d_{xz}(201\beta)$	85	2.44	509	0.347	2.05
	$\pi^*_{im}(201\alpha) \rightarrow \pi^*_{im}(203\alpha)$	8				
T_{25}	$\pi_{bim}(192\beta) \rightarrow d_{xz}+\pi^*_{im}(200\beta)$	45	2.94	422	0.096	2.14
	$\pi_{bim}(191\beta) \rightarrow d_{xz}+\pi^*_{im}(200\beta)$	36				
T_{29}	$\pi_{bim}(192\beta) \rightarrow \pi^*_{im}+d_{xz}(201\beta)$	34	3.09	402	0.070	2.34
	$\pi_{bim}(191\beta) \rightarrow \pi^*_{im}+d_{xz}(201\beta)$	24				

Table S16: Calculated vertical excitation energies (E^e), wavelengths (λ), oscillator strengths (f), eigen values of $\langle S^2 \rangle$ and singly-excited configurations of the main excited states in the visible range upon primary (singlet) and secondary photoexcitation (triplet) within the respective optimized equilibrium geometry of **Ru4** singly protonated at the 4*H*-imidazole. The MOs involved in the electronic transitions are depicted on Table S19.

Single protonation: Carbonyl group primary photoexcitation (singlet, S_0 geometry)						
q_i		ΔE / eV		ΔG / eV		
-0.655		2.01		2.01		
State	Transition	Weight / %	E^e / eV	λ / nm	f	$\langle S^2 \rangle$
S_3	$\pi_{bim}(199) \rightarrow \pi^*_{im}(201)$	47	1.00	1244	0.071	-
	$\pi_{bim}(200) \rightarrow \pi^*_{im}(201)$	42				
	$d_{xz}(197) \rightarrow \pi^*_{im}(201)$	10				
S_5	$d_{xz}(197) \rightarrow \pi^*_{im}(201)$	64	1.52	813	0.098	-
	$d_{xz}(198) \rightarrow \pi^*_{im}(201)$	22				
S_6	$\pi_{bim}(200) \rightarrow \pi^*_{im}(202)$	74	1.82	681	0.058	-
	$\pi_{bim}(199) \rightarrow \pi^*_{im}(202)$	19				
S_7	$\pi_{bim}(199) \rightarrow \pi^*_{im}(202)$	77	1.91	651	0.041	-
	$\pi_{bim}(200) \rightarrow \pi^*_{im}(202)$	18				
S_8	$d_{xz}(198) \rightarrow \pi^*_{im}(202)$	88	2.09	594	0.034	-
S_9	$d_{xz}(197) \rightarrow \pi^*_{im}(202)$	72	2.35	528	0.100	-
	$\pi_{im}(195) \rightarrow \pi^*_{im}(201)$	18				
S_{11}	$\pi_{bim}(200) \rightarrow \pi^*_{im}(203)$	67	2.49	499	0.176	-
	$\pi_{im}(195) \rightarrow \pi^*_{im}(201)$	14				
	$d_{yz}(196) \rightarrow \pi^*_{im}(202)$	10				
S_{12}	$\pi_{im}(195) \rightarrow \pi^*_{im}(201)$	52	2.59	479	0.483	-
	$\pi_{bim}(200) \rightarrow \pi^*_{im}(203)$	16				
	$d_{xz}(197) \rightarrow \pi^*_{im}(202)$	14				
S_{14}	$\pi_{bim}(194) \rightarrow \pi^*_{im}(201)$	96	2.72	456	0.048	-
S_{16}	$d_{xz}(198) \rightarrow \pi^*_{im}(203)$	83	2.79	444	0.096	-
S_{19}	$d_{xz}(197) \rightarrow \pi^*_{im}(203)$	83	3.03	409	0.075	-
secondary photoexcitation (triplet. T_1 geometry)						
State	Transition	Weight / %	E^e / eV	λ / nm	f	$\langle S^2 \rangle$
T_3	$\pi_{bim}(199\beta) \rightarrow \pi^*_{im}+d_{xz}(200\beta)$	79	0.98	1268	0.008	2.04
	$d_{xy}(196\beta) \rightarrow \pi^*_{im}+d_{xz}(200\beta)$	10				
T_4	$\pi_{bim}(198\beta) \rightarrow \pi^*_{im}+d_{xz}(200\beta)$	74	1.09	1140	0.023	2.04
	$d_{yz}(197\beta) \rightarrow \pi^*_{im}+d_{xz}(200\beta)$	11				
T_5	$\pi^*_{im}(201\alpha) \rightarrow \pi^*_{im}(202\alpha)$	80	1.19	1041	0.217	2.03
T_7	$\pi_{bim}(198\beta) \rightarrow d_{xz}+\pi^*_{im}(201\beta)$	68	1.49	830	0.094	2.06
	$\pi_{bim}(198\beta) \rightarrow \pi^*_{im}+d_{xz}(200\beta)$	10				
	$\pi^*_{im}(201\alpha) \rightarrow \pi^*_{im}(202\alpha)$	9				
T_8	$d_{yz}(197\beta) \rightarrow d_{xz}+\pi^*_{im}(201\beta)$	40	1.75	709	0.038	2.21
	$d_{yz}(197\beta) \rightarrow \pi^*_{im}+d_{xz}(200\beta)$	28				
	$\pi_{bim}(200\alpha) \rightarrow \pi^*_{im}(202\alpha)$	17				
	$\pi_{bim}(198\beta) \rightarrow d_{xz}+\pi^*_{im}(201\beta)$	8				
T_{10}	$d_{xy}(196\beta) \rightarrow d_{xz}+\pi^*_{im}(201\beta)$	48	1.81	685	0.025	2.16
	$d_{xy}(196\beta) \rightarrow \pi^*_{im}+d_{xz}(200\beta)$	37				
T_{12}	$\pi_{im}(195\beta) \rightarrow \pi^*_{im}+d_{xz}(200\beta)$	85	1.96	632	0.157	2.13
T_{15}	$\pi^*_{im}(201\alpha) \rightarrow \pi^*_{im}(203\alpha)$	75	2.30	540	0.077	2.25
	$\pi_{bim}(199\beta) \rightarrow \pi^*_{im}(202\beta)$	14				
T_{16}	$\pi_{im}(195\beta) \rightarrow d_{xz}+\pi^*_{im}(201\beta)$	77	2.40	517	0.256	2.20
T_{22}	$\pi_{bim}+\pi_{im}(194\beta) \rightarrow \pi^*_{im}+d_{xz}(200\beta)$	55	2.72	455	0.137	2.61
	$d_{yz}(197\beta) \rightarrow \pi^*_{im}(202\beta)$	13				
	$d_{xy}(197\alpha) \rightarrow \pi^*_{im}(202\alpha)$	10				
T_{26}	$\pi_{bim}(199\alpha) \rightarrow \pi^*_{im}(203\alpha)$	20	2.88	430	0.088	2.71
	$d_{xy}(196\beta) \rightarrow \pi^*_{im}(202\beta)$	18				
	$\pi^*_{im}(201\alpha) \rightarrow \pi^*_{im}(204\alpha)$	15				
T_{33}	$n_{im}(188\beta) \rightarrow \pi^*_{im}+d_{xz}(200\beta)$	22	3.07	404	0.064	2.12
	$\pi_{bim}+\pi_{im}(194\beta) \rightarrow d_{xz}+\pi^*_{im}(201\beta)$	22				
	$n_{bim}(189\beta) \rightarrow \pi^*_{im}+d_{xz}(200\beta)$	19				
T_{34}	$\pi_{bim}+\pi_{im}(194\beta) \rightarrow d_{xz}+\pi^*_{im}(201\beta)$	13	3.09	401	0.055	2.52
	$n_{im}(188\beta) \rightarrow \pi^*_{im}+d_{xz}(200\beta)$	12				
	$\pi_{bim}(198\beta) \rightarrow \pi^*_{im}(203\beta)$	11				
	$d_{xz}+\pi_{bim}(195\alpha) \rightarrow \pi^*_{im}(202\alpha)$	10				
	$n_{bim}(190\beta) \rightarrow \pi^*_{im}+d_{xz}(200\beta)$	9				

Table S17: Calculated vertical excitation energies (E^e), wavelengths (λ), oscillator strengths (f), eigen values of $\langle s^2 \rangle$ and singly-excited configurations of the main excited states in the visible range upon primary (singlet) and secondary photoexcitation (triplet) within the

respective optimized equilibrium geometry of **Ru4** singly protonated at the carbonyl group. The MOs involved in the electronic transitions are depicted on Table S20.

Single protonation: Biimidazole
primary photoexcitation (singlet. S_0 geometry)

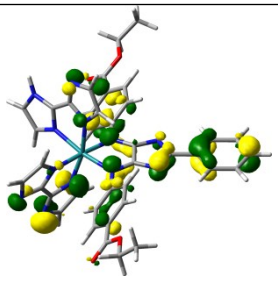
$\pi_{delocal}(193)$

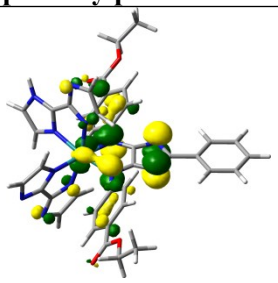
$\pi_{im}(195)$

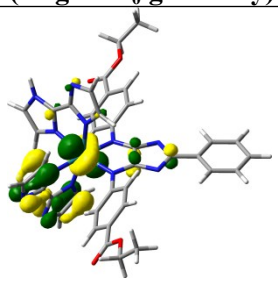
$d_{yz}+\pi_{bim}(197)$

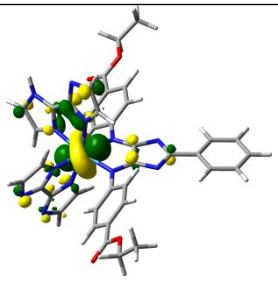
$d_{yz}+\pi_{bim}(198)$

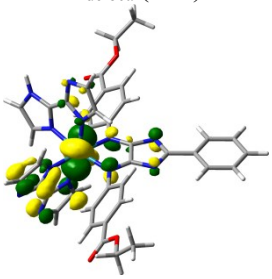
$d_{xz}(199)$

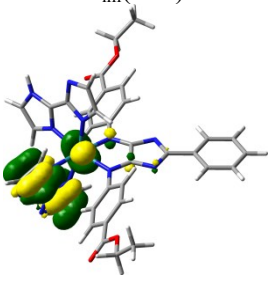
$\pi_{bim}(200)$

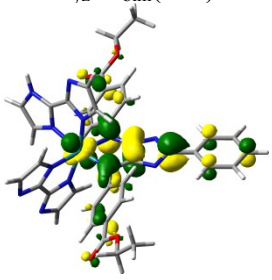
$\pi^*_{im}(201)$

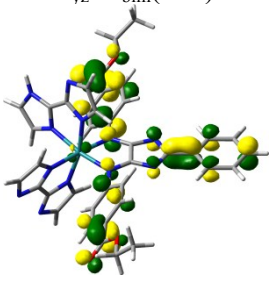
$\pi^*_{im}(203)$

secondary photoexcitation (triplet. T_1 geometry)

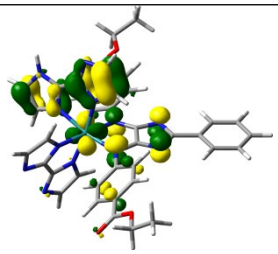
(198α)

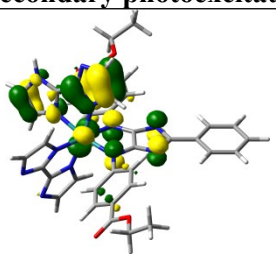
(199α)

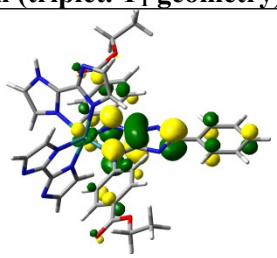
$\pi^*_{im}(201\alpha)$

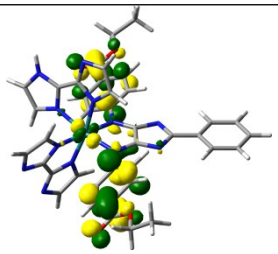
$\pi^*_{im}(202\alpha)$

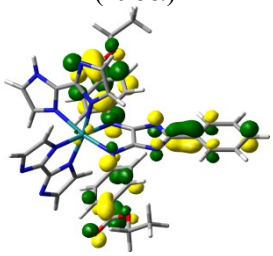
$\pi^*_{im}(203\alpha)$

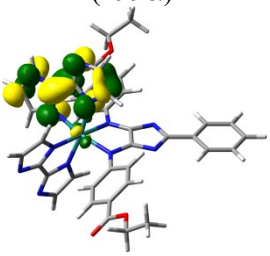
$\pi^*_{bim}(204\alpha)$

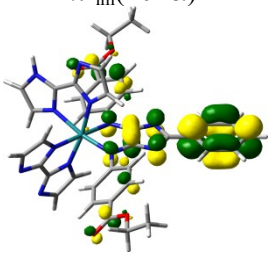
$\pi^*_{im}(205\alpha)$

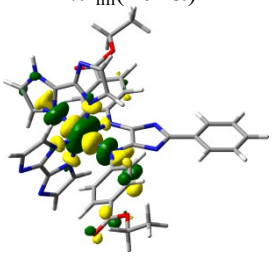
$d_{z^2}(209\alpha)$

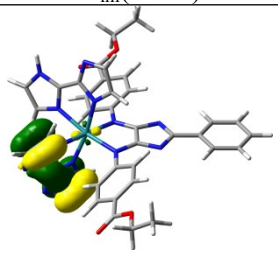
$\pi_{bim}(193\beta)$

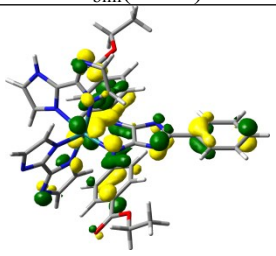
$\pi_{im}(194\beta)$

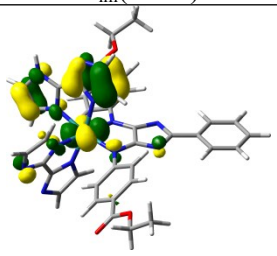
$\pi_{bim}+d_{yz}(195\beta)$

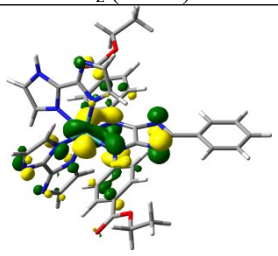
$\pi_{im}(196\beta)$

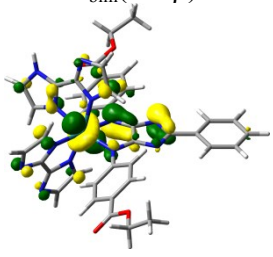
$d_{yz}+\pi_{im}(197\beta)$

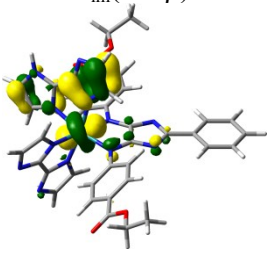
$d_{xy}+\pi_{bim}(198\beta)$

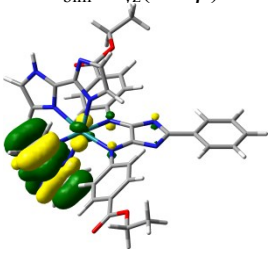
$\pi_{bim}(199\beta)$

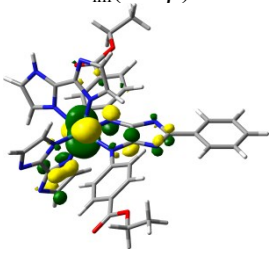
$d_{xz}(200\beta)$

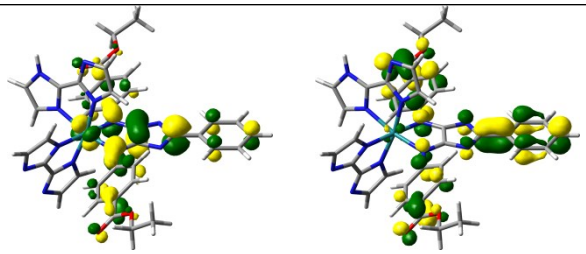

$\pi^*_{im}(201\beta)$ $\pi^*_{im}(203\beta)$

Table S18: MOs involved in the bright singlet and triplet excited states (Table S15) of **Ru4**, singly protonated at the biimidazole, upon primary and secondary photoexcitation.

Single protonation: 4*H*-imidazole
primary photoexcitation (singlet. S_0 geometry)

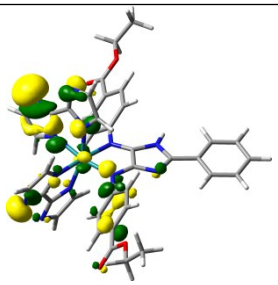
$n_{bim}(190)$

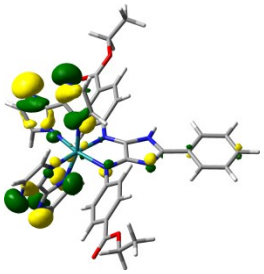
$n_{bim}(191)$

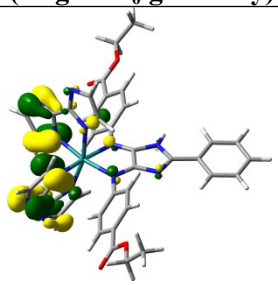
$\pi_{bim}(192)$

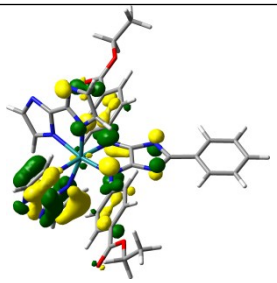
$\pi_{delocal}(193)$

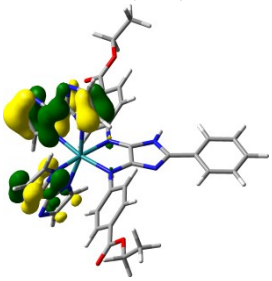
$\pi_{bim}(194)$

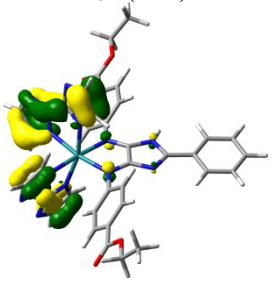
$\pi_{bim}(195)$

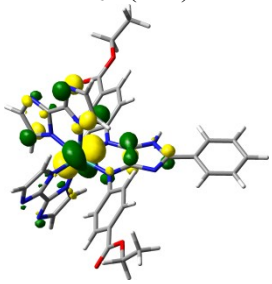
$d_{xy}(196)$

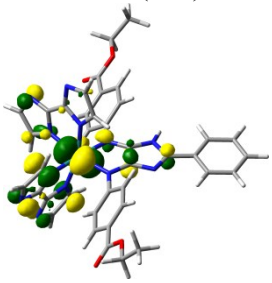
$d_{yz}(197)$

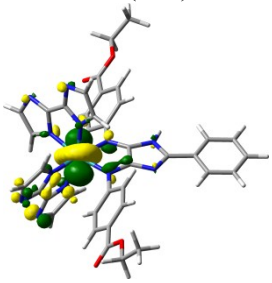
$d_{xz}(198)$

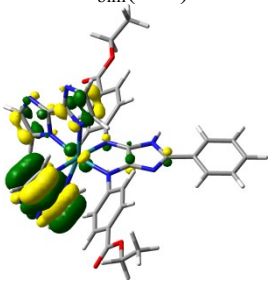
$\pi_{bim}(199)$

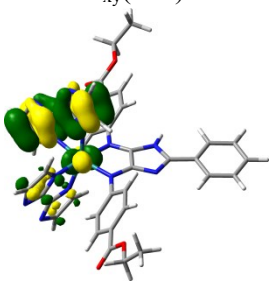
$\pi_{bim}(200)$

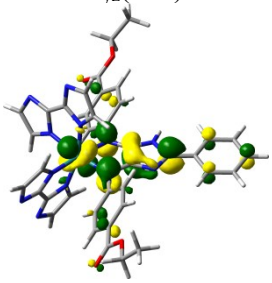
$\pi^*_{im}(201)$

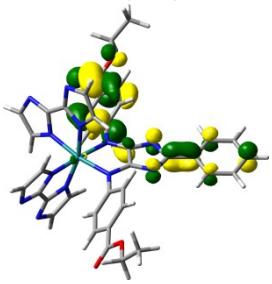
$\pi^*_{im}(202)$

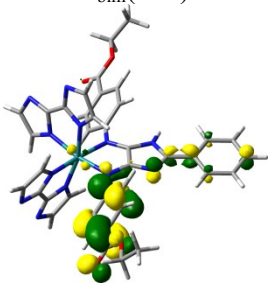
$\pi^*_{im}(203)$

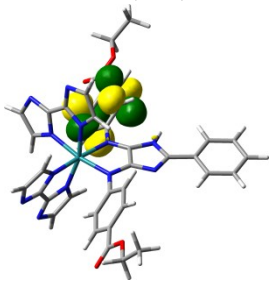
$\pi^*_{im}(205)$

secondary photoexcitation (triplet. T_1 geometry)

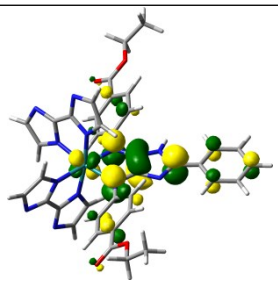
$\pi^*_{im}(201\alpha)$

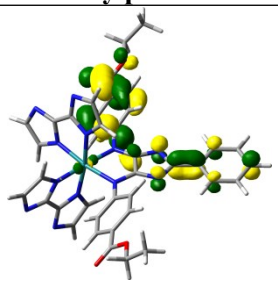
$\pi^*_{im}(202\alpha)$

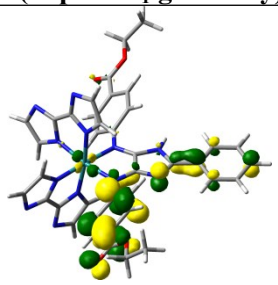
$\pi^*_{im}(203\alpha)$

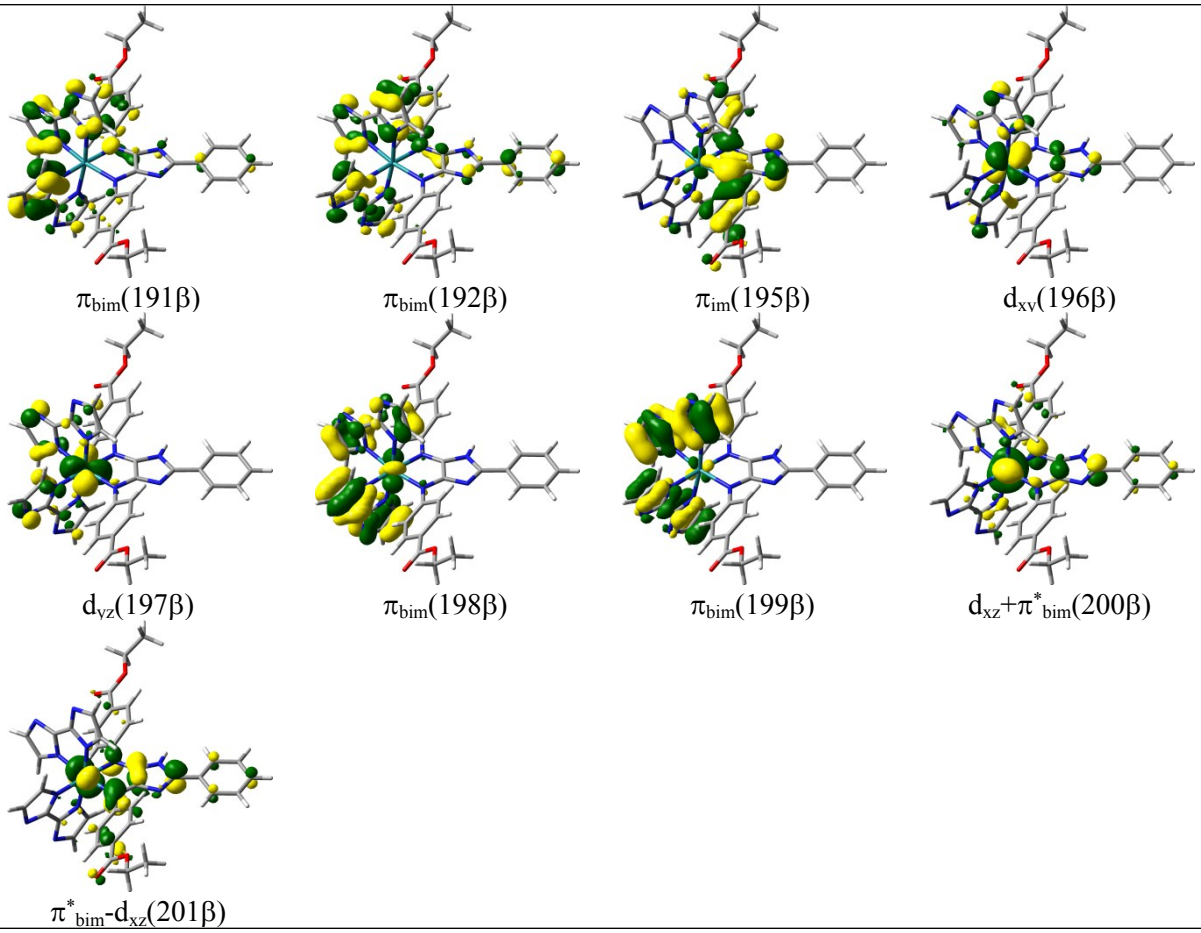

Table S19: MOs involved in the bright singlet and triplet excited states (Table S16) of **Ru4**, singly protonated at the 4*H*-imidazole, upon primary and secondary photoexcitation.

Single protonation: Carbonyl group
primary photoexcitation (singlet. S_0 geometry)

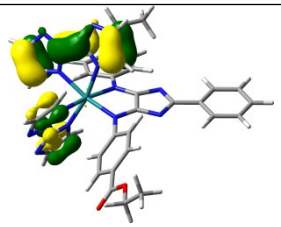
$\pi_{bim}(194)$

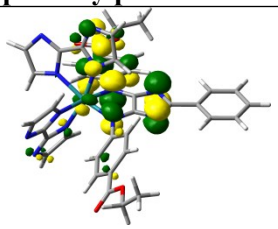
$\pi_{im}(195)$

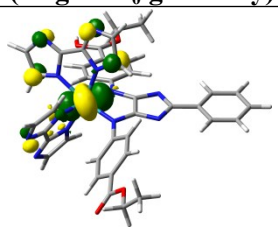
$d_{yz}(196)$

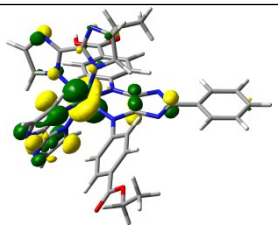
$d_{xz}(197)$

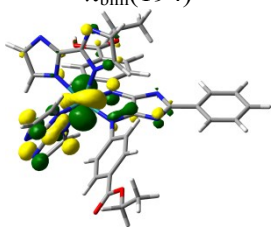
$d_{xy}(198)$

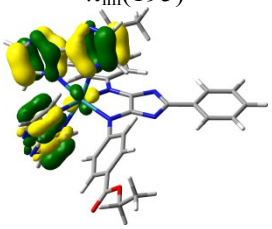
$\pi_{bim}(199)$

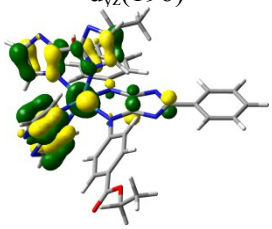
$\pi_{bim}(200)$

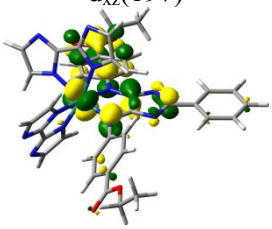
$\pi^*_{im}(201)$

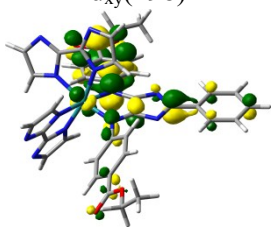
$\pi^*_{im}(202)$

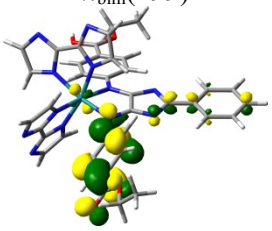
$\pi^*_{im}(203)$

secondary photoexcitation (triplet. T_1 geometry)

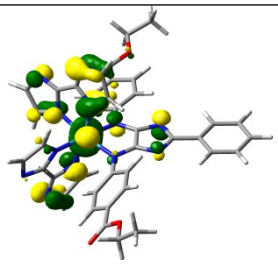
$d_{xz}+\pi_{bim}(195\alpha)$

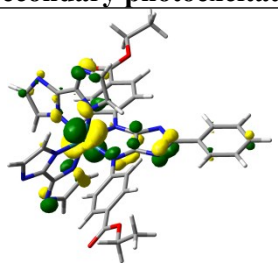
$d_{xy}(197\alpha)$

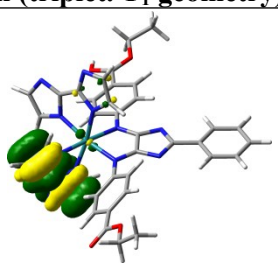
$\pi_{bim}(199\alpha)$

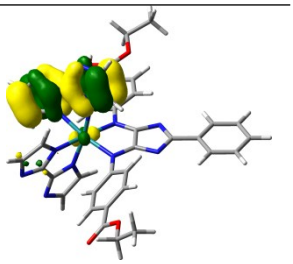
$\pi_{bim}(200\alpha)$

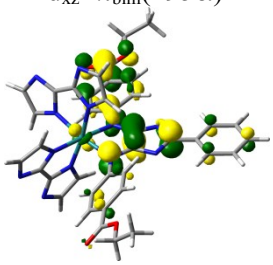
$\pi_{im}^*(201\alpha)$

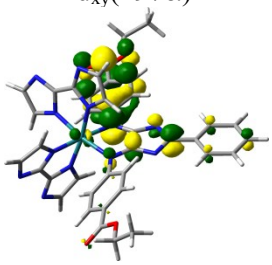
$\pi_{im}^*(202\alpha)$

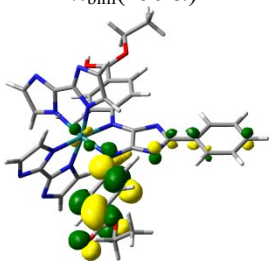
$\pi_{im}^*(203\alpha)$

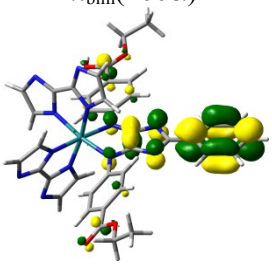
$\pi_{im}^*(204\alpha)$

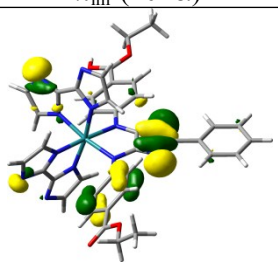
$n_{im}(188\beta)$

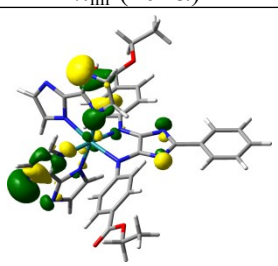
$n_{bim}(189\beta)$

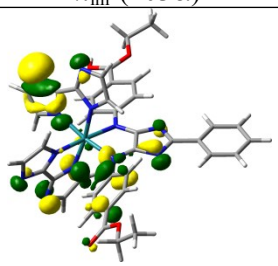
$n_{bim}(190\beta)$

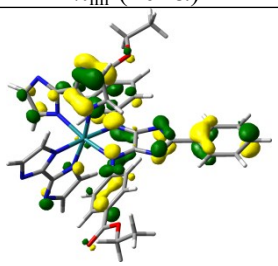
$\pi_{bim}+\pi_{im}(194\beta)$

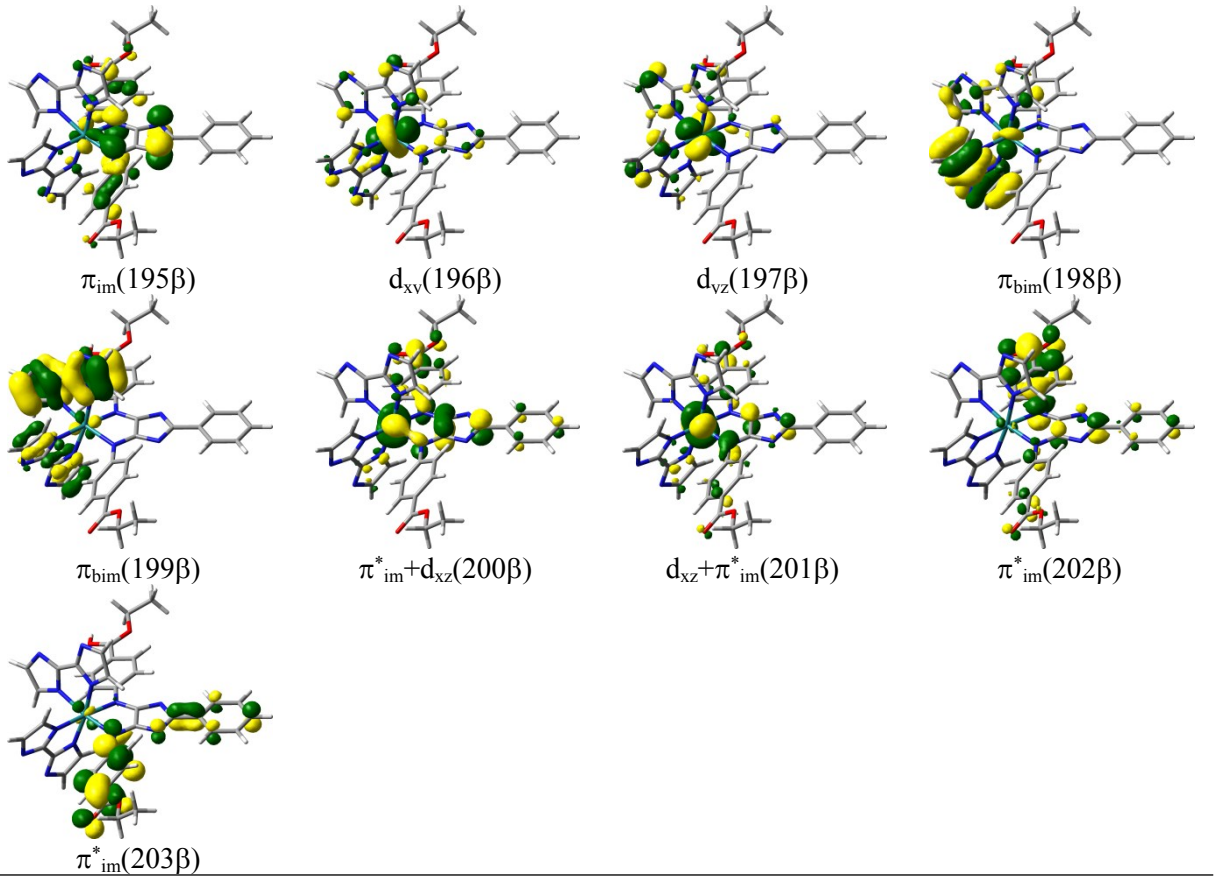

Table S20: MOs involved in the bright singlet and triplet excited states (Table S17) of **Ru4**, singly protonated at the carbonyl group, upon primary and secondary photoexcitation.

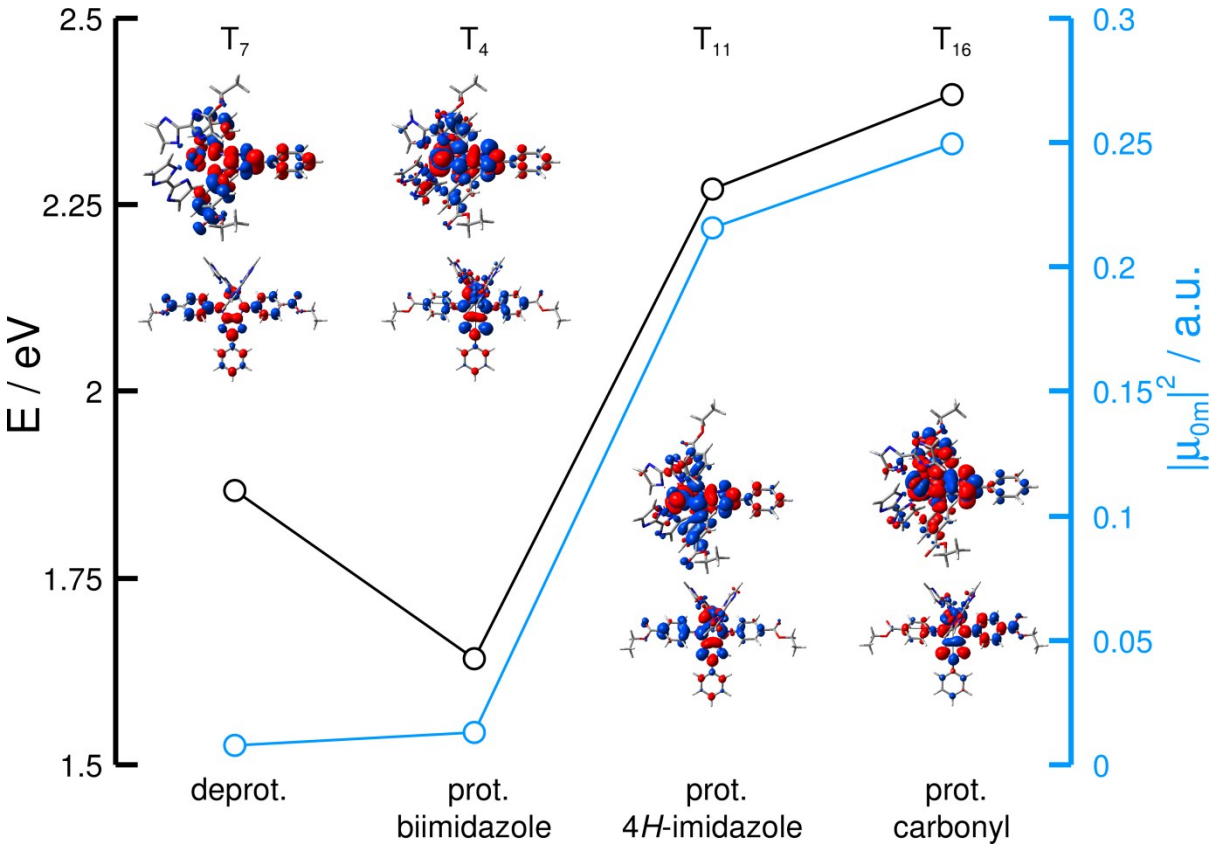

Figure S5: Excitation energies and square of the absolute value of the transition dipole moments for the excitations into T_7 (deprot.), T_4 (prot. biimidazole), T_{11} (prot. 4*H*-imidazole) and T_{16} (prot. carbonyl) of the deprotonated and the three singly protonated forms of **Ru4**.